The Astronomical Journal, 129:1669–1685, 2005 March

CHROMOSPHERICALLY ACTIVE STARS. XXIV. THE GIANT, SINGLE-LINED BINARIES HD 37824, HD 181809, AND HD 217188

Francis C. Fekel[1,2] and Gregory W. Henry[2]
Center of Excellence in Information Systems, Tennessee State University, 330 10th Avenue North, Nashville, TN 37203;
fekel@evans.tsuniv.edu, henry@schwab.tsuniv.edu
Received 2004 July 9; accepted 2004 November 22

ABSTRACT

We have obtained spectroscopy and photometry of three chromospherically active, single-lined spectroscopic binaries, HD 37824 (V1149 Ori), HD 181809 (V4138 Sgr), and HD 217188 (AZ Psc). HD 37824 has a circular orbit with a period of 53.57 days. Its primary is a K0 III star, while the secondary is likely a G or K dwarf. HD 181809 has an orbit with a period of 13.04667 days and a low eccentricity of 0.040. The primary has a spectral type of K0 III–IV, and its secondary is probably an M dwarf. The orbit of HD 217188 has a period of 47.1209 days and a moderately high eccentricity of 0.470. The spectral type of the primary is K0 III, while the secondary is likely an M dwarf. All three systems are estimated to have near solar iron abundances. Photometric observations spanning 15–16 years for all three stars yield mean photometric periods of 53.12, 59.85, and 90.89 days for HD 37824, HD 181809, and HD 217188, respectively. Thus, HD 37824 is rotating synchronously with the orbital period, while HD 181809 and HD 217188 are both rotating considerably slower than synchronously. All three stars show long-term variations in mean brightness and photometric amplitude, but no correlations are observed between the seasonal mean brightness, photometric amplitude, and seasonal photometric period in any of the stars. No clear evidence for long-term periodic variations in any of these parameters is present. The circular orbit of HD 37824 and the synchronous rotation of its K giant argue that the star is in the core helium-burning phase of its evolution. The giant components of HD 181809 and HD 217188 are asynchronous rotators, and both systems have eccentric orbits. Thus, those two stars are likely first-ascent giants.

Key words: binaries: spectroscopic — stars: spots — stars: variables: other

Online material: machine-readable tables

1. INTRODUCTION

Chromospherically active stars have been identified in spectroscopic surveys by their strong Ca II H and K emission. In particular, such active stars have been found in objective-prism surveys (e.g., Bidelman & MacConnell 1973; Bidelman 1981, 1985) and more recently in the moderate- and high-resolution spectroscopic searches of Henry et al. (1996) and Strassmeier et al. (2000), respectively. Over the past several decades, satellite surveys at X-ray and ultraviolet wavelengths have provided another very effective way of finding active, late-type stars. The observations produced by satellites such as *HEAO-1*, *Einstein*, *EXOSAT*, the *Extreme Ultraviolet Explorer* (*EUVE*), and *ROSAT* have led to optical identifications (e.g., Buckley et al. 1987; Fleming et al. 1989; Cutispoto et al. 1991, 1999; Tagliaferri et al. 1994; Jeffries et al. 1995; Neuhaüser et al. 1997) of many chromospherically active stars. Here we discuss three stars discovered from objective-prism spectra (Bidelman & MacConnell 1973; Bidelman 1981). Although spectroscopic orbits have been determined previously for HD 37824, HD 181809, and HD 217188, our new results improve their orbital elements. We also analyze our extensive photometric observations and, using complementary spectroscopy and photometry, discuss the nature of the systems.

2. SPECTROSCOPIC OBSERVATIONS AND REDUCTIONS

From 1979 November to 2003 September we obtained 60 high-resolution spectrograms of HD 37824. The radial velocities of the first 11, obtained at McDonald Observatory and Kitt Peak National Observatory (KPNO) were published previously by Fekel et al. (1986). The remaining observations were acquired with the KPNO coudé feed telescope, coudé spectrograph, and a TI CCD detector. All but five of the KPNO spectrograms are centered in the red at 6430 Å, cover a wavelength range of about 80 Å, and have a resolution of 0.21 Å. Two observations were obtained of the Hα region and three of the lithium region around 6708 Å. The spectrograms of these latter two regions have the same wavelength range and resolution as the spectrograms obtained in the 6430 Å region. Typical signal-to-noise ratios are 150–200.

From 1979 November to 2003 October we collected 54 high-resolution spectrograms of HD 181809. The radial velocities for the first five, which were acquired at McDonald Observatory, were published by Fekel et al. (1986). Our additional spectrograms were all obtained with the previously mentioned KPNO telescope, spectrograph, and detector system. Except for one centered at Hα and one in the lithium region, all the KPNO spectrograms are centered at 6430 Å.

From 1981 August to 2002 September we obtained 52 high-resolution spectrograms of HD 217188. Fekel et al. (1986) listed the radial velocities for the first six observations, which were obtained at McDonald Observatory and KPNO. Our additional spectrograms were acquired at KPNO with the same telescope, spectrograph, and detector combination as the observations of

[1] Visiting Astronomer, Kitt Peak National Observatory, National Optical Astronomy Observatory, operated by the Association of Universities for Research in Astronomy, Inc., under cooperative agreement with the National Science Foundation.
[2] Also Senior Research Associate, Department of Physics and Astronomy, Vanderbilt University, Nashville, TN 37235.

HD 37824. Two of the spectrograms are centered at Hα and one at the lithium region; the rest are of the usual 6430 Å region.

Our previously published velocities of these three stars have been revised slightly because different velocities have been adopted for the standard stars (Scarfe et al. 1990). The radial velocities for our more recent spectra were determined with the IRAF cross-correlation program *fxcor* (Fitzpatrick 1993). The cross-correlation reference stars for the spectra of HD 37824 were primarily the IAU velocity standards HR 1283, β Gem, and HR 3145. Their adopted velocities are 24.8, 3.2, and 71.4 km s^{-1}, respectively, from Scarfe et al. (1990). For HD 181809 we used β Aql as the reference star. A velocity of -40.2 km s^{-1}, measured relative to the IAU velocity standard HR 7560, was adopted for it from our unpublished results. Finally, for HD 217188 we used primarily β Aql, although a few spectra were cross-correlated against the IAU velocity standards α Ari or HR 8551. The latter two stars have velocities of -14.5 and 54.3 km s^{-1}, respectively (Scarfe et al. 1990). All the individual radial velocities for HD 37824, HD 181809, and HD 217188 are given in Tables 1, 2, and 3, respectively, along with their corresponding orbital phases and velocity residuals computed from the orbits determined in §§ 4.2, 5.2, and 6.2.

Several computer programs were used to determine the orbital elements. With an adopted period, preliminary orbital elements sometimes were computed with BISP (Wolfe et al. 1967), a computer program that uses a slightly modified version of the Wilsing-Russell method. With these or other well-determined elements, the orbit was refined with SB1 (Barker et al. 1967), a program that uses differential corrections. If the eccentricity was low, a circular orbit with SB1C (D. Barlow 1998, private communication), which also uses differential corrections to determine the orbital elements, was computed.

3. PHOTOMETRIC OBSERVATIONS AND REDUCTIONS

Our photometric observations were all obtained with the T3 0.4 m automatic photoelectric telescope (APT) at Fairborn Observatory in southern Arizona. The 0.4 m APT uses a temperature-stabilized EMI 9924B photomultiplier tube to acquire data successively through Johnson B and V filters. Each program star was measured each clear night in the following sequence, termed a group observation: K, S, C, V, C, V, C, V, C, S, K, in which K is a check star, C is the comparison star, V is the program star, and S is a sky reading. Three $V - C$ and two $K - C$ differential magnitudes were formed from each sequence and averaged together to create group means. Group mean differential magnitudes with internal standard deviations greater than 0.01 mag were rejected to filter the observations taken under nonphotometric conditions. The surviving group means were corrected for differential extinction with nightly extinction coefficients, transformed to the Johnson system with yearly mean transformation coefficients, and treated as single observations thereafter. The external precision of these group means, based on standard deviations for pairs of constant stars, is typically $\sim$0.004–0.005 mag on good nights with this telescope. Prior to 1992, when a new precision photometer was installed on the telescope, the precision of the observations was approximately 0.012 mag. Further information on the operation of our APTs can be found in Henry (1995a, 1995b, 1999) and Eaton et al. (2003).

The T3 APT acquired 1271 good group means in V and 1317 in B for HD 37824 during 15 observing seasons between 1988 September and 2003 April. The individual group mean $V - C$ and $K - C$ differential magnitudes are given in Table 4. The

TABLE 1

RADIAL VELOCITIES OF HD 37824

HJD − 2,400,000	Phase	Velocity (km s^{-1})	$O - C$ (km s^{-1})	Weight	Source[a]
43,940.336	0.558	2.9	−0.5	0.05	SAAO
43,941.336	0.576	2.6	−2.0	0.05	SAAO
43,944.351	0.633	9.1	−1.2	0.05	SAAO
43,945.355	0.651	12.7	0.0	0.05	SAAO
43,969.226	0.097	51.6	1.8	0.05	SAAO
43,971.225	0.134	46.4	0.7	0.05	SAAO
43,973.244	0.172	34.4	−6.2	0.05	SAAO
43,976.220	0.228	34.2	2.4	0.05	SAAO
43,977.213	0.246	26.6	−2.2	0.05	SAAO
43,978.216	0.265	26.2	0.5	0.05	SAAO
43,979.223	0.284	25.4	2.8	0.05	SAAO
43,980.214	0.302	20.3	0.7	0.05	SAAO
44,178.918	0.011	54.0	−0.5	1.00	McD
44,182.011	0.069	50.0	−2.2	0.00	McD
44,235.519	0.068	4.6	−47.7	0.00	SAAO
44,239.457	0.141	46.8	1.9	0.05	SAAO
44,241.417	0.178	37.3	−2.5	0.05	SAAO
44,245.368	0.251	28.7	0.8	0.05	SAAO
44,246.375	0.270	26.7	1.9	0.05	SAAO
44,297.342	0.221	31.8	−1.0	0.05	SAAO
44,298.280	0.239	25.2	−4.7	0.05	SAAO
44,299.287	0.258	29.5	2.7	0.05	SAAO
44,300.280	0.276	25.3	1.5	0.05	SAAO
44,301.274	0.295	20.1	−0.6	0.05	SAAO
44,302.275	0.314	21.1	3.3	0.05	SAAO
44,332.246	0.873	43.5	−3.1	0.05	SAAO
44,333.260	0.892	47.7	−1.0	0.05	SAAO
44,335.256	0.929	49.6	−2.4	0.05	SAAO
44,336.266	0.948	51.5	−1.7	0.05	SAAO
44,337.246	0.966	60.0	6.0	0.05	SAAO
44,364.226	0.470	6.0	3.9	0.05	SAAO
44,535.524	0.667	13.0	−2.0	0.05	SAAO
44,536.591	0.687	20.2	2.3	0.05	SAAO
44,537.607	0.706	17.4	−3.5	0.05	SAAO
44,538.605	0.725	21.8	−2.1	0.05	SAAO
44,539.595	0.743	25.9	−1.1	0.05	SAAO
44,590.485	0.693	18.7	−0.2	0.05	SAAO
44,592.319	0.727	22.7	−1.7	0.05	SAAO
44,592.601	0.733	24.2	−1.0	0.05	SAAO
44,593.310	0.746	24.1	−3.3	0.05	SAAO
44,593.593	0.751	29.2	0.9	0.05	SAAO
44,595.412	0.785	32.7	−1.2	0.05	SAAO
44,596.329	0.802	33.8	−2.9	0.05	SAAO
44,596.599	0.807	38.4	1.0	0.05	SAAO
44,626.734	0.370	9.3	−0.7	1.00	McD
44,627.801	0.390	7.8	0.1	1.00	McD
44,639.306	0.604	−12.4	−19.5	0.00	SAAO
44,692.240	0.592	5.2	−0.8	0.05	SAAO
44,693.231	0.611	3.2	−4.6	0.05	SAAO
44,694.227	0.630	11.5	1.6	0.05	SAAO
44,707.208	0.872	43.2	−3.3	0.05	SAAO
44,895.019	0.377	9.4	0.3	1.00	McD
45,357.779	0.015	55.3	0.8	1.00	KPNO
45,359.811	0.053	52.1	−1.1	1.00	KPNO
45,360.789	0.071	51.8	−0.2	1.00	KPNO
45,361.721	0.089	50.1	−0.5	1.00	KPNO
45,719.854	0.773	31.5	−0.5	1.00	KPNO
45,812.616	0.505	1.3	−0.3	1.00	KPNO
48,163.022	0.377	9.4	0.2	1.00	KPNO
48,167.996	0.469	1.1	−1.0	1.00	KPNO
48,346.594	0.803	35.7	−1.1	1.00	KPNO
48,573.025	0.029	54.5	0.3	1.00	KPNO
48,577.017	0.104	49.7[b]	0.5	1.00	KPNO
48,577.881	0.120	48.6[c]	1.2	1.00	KPNO

TABLE 1—*Continued*

HJD − 2,400,000	Phase	Velocity (km s^{-1})	$O-C$ (km s^{-1})	Weight	Source[a]
48,604.876	0.624	9.9	0.6	1.00	KPNO
48,606.733	0.659	14.4	0.7	1.00	KPNO
49,245.985	0.591	6.0	0.2	1.00	KPNO
49,248.025	0.629	10.1	0.3	1.00	KPNO
49,250.034	0.666	15.6	0.8	1.00	KPNO
49,307.882	0.746	26.9	−0.5	1.00	KPNO
49,674.838	0.595	6.2	0.0	1.00	KPNO
49,834.615	0.578	4.3	−0.4	1.00	KPNO
49,971.005	0.124	45.6[b]	−1.4	1.00	KPNO
49,972.004	0.142	44.9	0.2	1.00	KPNO
49,973.030	0.161	41.5[c]	−0.6	1.00	KPNO
49,974.028	0.180	39.4	0.0	1.00	KPNO
50,363.947	0.458	2.3	−0.2	1.00	KPNO
50,399.952	0.130	46.4	0.2	1.00	KPNO
50,400.963	0.149	43.9[c]	0.1	1.00	KPNO
50,401.889	0.166	41.6	0.2	1.00	KPNO
50,405.006	0.224	32.6	0.2	1.00	KPNO
50,754.932	0.756	28.9	−0.2	1.00	KPNO
50,757.928	0.812	38.4	0.2	1.00	KPNO
50,758.939	0.831	41.1	0.1	1.00	KPNO
50,829.794	0.153	42.5	−0.7	1.00	KPNO
50,830.749	0.171	40.5	−0.2	1.00	KPNO
50,831.681	0.188	37.7	−0.4	1.00	KPNO
50,832.763	0.209	34.4	−0.5	1.00	KPNO
50,833.766	0.227	31.4	−0.5	1.00	KPNO
50,926.630	0.961	54.5	0.7	1.00	KPNO
50,927.617	0.979	54.9	0.5	1.00	KPNO
50,928.616	0.998	55.1	0.5	1.00	KPNO
51,303.618	0.997	54.7	0.1	1.00	KPNO
51,472.952	0.158	42.3	−0.3	1.00	KPNO
51,473.933	0.176	39.6	−0.3	1.00	KPNO
51,474.985	0.196	37.0	0.1	1.00	KPNO
51,476.993	0.234	30.2	−0.6	1.00	KPNO
51,803.011	0.319	17.0	0.0	1.00	KPNO
51,803.994	0.337	14.4	0.1	1.00	KPNO
52,013.622	0.250	28.7	0.6	1.00	KPNO
52,014.628	0.269	25.6	0.6	1.00	KPNO
52,015.601	0.287	22.8	0.8	1.00	KPNO
52,016.602	0.306	19.6	0.6	1.00	KPNO
52,017.607	0.324	16.8	0.6	1.00	KPNO
52,902.966	0.850	43.8	0.1	1.00	KPNO
52,903.980	0.869	46.4	0.3	1.00	KPNO
52,904.977	0.888	48.4	0.1	1.00	KPNO

[a] SAAO: South African Astronomical Observatory; McD: McDonald Observatory; KPNO: Kitt Peak National Observatory.
[b] Hα region, central wavelength 6560 Å.
[c] Lithium region, central wavelength 6700 Å.

photometric comparison star was HD 38309 ($V = 6.09$, $B-V = 0.320$, F0 III), while the check star was HD 37984 (51 Ori, HR 1963; $V = 4.90$, $B-V = 1.144$, K1 III).

A total of 1012 good group means in V and 1040 in B were acquired for HD 181809 during 16 observing seasons between 1988 April and 2003 July. The individual $V-C$ and $K-C$ differential magnitudes are given in Table 5. The comparison star was HD 182629 ($V = 5.57$, $B-V = 1.228$, K1–K2 III), while the check star was HD 181240 (HR 7327; $V = 5.59$, $B-V = 0.276$, A6).

Finally, the APT acquired 1110 good group means in V and 1105 in B for HD 217188 during 15 observing seasons between 1988 May and 2003 July. The individual $V-C$ and $K-C$ differential magnitudes are given in Table 6. The comparison star was HD 217428 (3 Psc, HR 8750; $V = 6.62$,

TABLE 2

Radial Velocities of HD 181809

HJD − 2,400,000	Phase	Velocity (km s^{-1})	$O-C$ (km s^{-1})	Source[a]
44,180.583	0.596	−18.6[b]	−4.1	McD
44,473.759	0.067	−11.4	0.3	McD
44,474.669	0.137	−16.3	0.0	McD
44,480.736	0.602	−14.0	0.2	McD
44,894.566	0.321	−21.9[b]	1.5	McD
46,582.944	0.730	−7.0	0.1	KPNO
47,823.577	0.821	−3.2[c]	0.9	KPNO
48,576.624	0.540	−17.4	0.2	KPNO
48,914.569	0.443	−22.0	−0.2	KPNO
49,245.631	0.818	−4.2	0.0	KPNO
49,248.608	0.046	−10.3	0.1	KPNO
49,301.560	0.105	−13.8	0.4	KPNO
49,460.011	0.250	−21.7	0.2	KPNO
49,463.974	0.553	−16.9	0.0	KPNO
49,621.621	0.637	−12.4	−0.2	KPNO
49,622.640	0.715	−7.9	0.0	KPNO
49,674.565	0.695	−8.8	0.1	KPNO
49,677.546	0.923	−4.8[d]	−0.3	KPNO
49,899.827	0.960	−6.0	−0.2	KPNO
49,900.879	0.041	−9.9	0.2	KPNO
49,968.645	0.235	−21.5	−0.1	KPNO
49,969.656	0.313	−23.4	0.0	KPNO
49,970.662	0.390	−23.0	0.1	KPNO
49,971.689	0.468	−20.9	0.0	KPNO
49,972.603	0.539	−17.7	0.0	KPNO
49,973.677	0.621	−13.0	0.1	KPNO
50,199.011	0.892	−4.0	−0.1	KPNO
50,199.985	0.967	−5.8	0.2	KPNO
50,203.967	0.272	−22.7	−0.1	KPNO
50,262.807	0.782	−5.3	−0.2	KPNO
50,263.895	0.865	−3.5	0.2	KPNO
50,265.919	0.020	−9.1	−0.3	KPNO
50,361.583	0.353	−23.5	0.0	KPNO
50,362.623	0.432	−22.2	0.0	KPNO
50,363.624	0.509	−18.7	0.5	KPNO
50,630.867	0.993	−7.6	−0.3	KPNO
50,632.890	0.148	−17.2	−0.2	KPNO
50,635.830	0.373	−23.8	−0.4	KPNO
50,637.830	0.526	−18.4	−0.1	KPNO
50,719.625	0.796	−5.0	−0.3	KPNO
50,720.634	0.873	−4.0	−0.2	KPNO
50,721.584	0.946	−5.2	0.0	KPNO
50,754.551	0.473	−21.0	−0.2	KPNO
50,756.552	0.626	−13.1	−0.3	KPNO
50,757.564	0.704	−8.9	−0.5	KPNO
51,089.593	0.153	−17.6	−0.3	KPNO
51,091.610	0.307	−23.1	0.2	KPNO
51,094.571	0.534	−17.9	0.0	KPNO
51,303.972	0.584	−15.1	0.1	KPNO
51,304.948	0.659	−10.9	0.0	KPNO
52,181.610	0.853	−3.5	0.3	KPNO
52,902.650	0.119	−15.2	−0.1	KPNO
52,903.627	0.194	−19.5	0.1	KPNO
52,942.559	0.178	−18.6	0.1	KPNO

[a] McD: McDonald Observatory; KPNO: Kitt Peak National Observatory.
[b] Velocity given zero weight.
[c] Lithium region, central wavelength 6700 Å.
[d] Hα region, central wavelength 6560 Å.

TABLE 3
RADIAL VELOCITIES OF HD 217188

HJD − 2,400,000	Phase	Velocity (km s^{-1})	$O - C$ (km s^{-1})	Source[a]
44,832.924	0.568	−26.9	−1.0	McD
44,894.736	0.880	−17.3	−0.1	McD
45,358.592	0.724	−25.4[b]	−1.3	KPNO
45,594.897	0.739	−23.9	−0.1	KPNO
45,941.884	0.102	−15.4	−0.3	KPNO
45,974.807	0.801	−21.5	0.3	KPNO
46,972.959	0.984	−4.8	1.1	KPNO
47,383.602	0.699	−24.7	−0.1	Coravel
47,392.614	0.890	−16.5	−0.2	Coravel
47,395.488	0.951	−9.6	−0.2	Coravel
47,418.476	0.439	−25.7	0.2	Coravel
47,451.388	0.137	−17.8	0.2	Coravel
47,453.847	0.189	−20.9	0.1	KPNO
47,492.267	0.005	−6.1	−0.7	Coravel
47,728.588	0.020	−5.8	0.2	Coravel
47,733.592	0.126	−17.3	−0.1	Coravel
47,737.614	0.211	−21.7	0.2	Coravel
47,743.606	0.339	−25.0	0.0	Coravel
47,748.537	0.443	−25.7	0.2	Coravel
47,753.538	0.549	−26.4	−0.4	Coravel
47,758.575	0.656	−25.2	0.0	Coravel
47,761.537	0.719	−24.2	0.0	Coravel
47,772.481	0.951	−9.5	−0.2	Coravel
47,774.501	0.994	−5.2	0.2	Coravel
47,822.317	0.009	−6.4	−0.9	Coravel
47,841.280	0.411	−25.6	0.1	Coravel
47,854.279	0.687	−24.8	0.0	Coravel
47,858.310	0.773	−22.8	0.1	Coravel
48,108.569	0.084	−13.0	0.1	Coravel
48,110.551	0.126	−17.0	0.2	Coravel
48,113.551	0.190	−21.1	−0.1	Coravel
48,117.579	0.275	−23.8	0.0	Coravel
48,146.479	0.888	−16.1	0.4	Coravel
48,150.413	0.972	−6.8	0.1	Coravel
48,152.488	0.016	−5.0	0.8	Coravel
48,155.425	0.078	−12.3	0.2	Coravel
48,162.816	0.235	−22.7	0.0	KPNO
48,167.761	0.340	−24.0	1.0	KPNO
48,223.269	0.518	−26.2	−0.2	Coravel
48,225.267	0.560	−26.3	−0.4	Coravel
48,226.275	0.582	−25.9	0.0	Coravel
48,505.783	0.513	−26.1	−0.1	KPNO
48,572.699	0.934	−11.6	0.0	KPNO
48,576.650	0.017	−5.8	0.1	KPNO
48,577.643	0.038	−8.0[c]	−0.3	KPNO
48,604.624	0.611	−25.6	0.1	KPNO
48,774.965	0.226	−22.5	0.0	KPNO
48,912.848	0.152	−19.0	0.0	KPNO
49,245.762	0.217	−22.1	0.1	KPNO
49,619.802	0.155	−19.6	−0.4	KPNO
49,622.745	0.218	−22.2	0.0	KPNO
49,677.640	0.383	−25.5[d]	0.0	KPNO
49,678.728	0.406	−25.8	−0.1	KPNO
49,969.826	0.583	−26.0	−0.2	KPNO
49,971.776	0.625	−25.7	−0.1	KPNO
49,973.693	0.665	−24.9	0.2	KPNO
50,265.945	0.868	−18.2	−0.1	KPNO
50,361.685	0.899	−15.4	0.0	KPNO
50,362.748	0.922	−13.2	−0.2	KPNO
50,363.719	0.943	−10.6	−0.2	KPNO
50,364.716	0.964	−8.2	−0.4	KPNO
50,365.687	0.984	−5.7	0.2	KPNO
50,366.650	0.005	−4.9	0.5	KPNO
50,404.618	0.811	−21.3[d]	0.1	KPNO
50,634.921	0.698	−24.5	0.1	KPNO
50,637.871	0.761	−22.9	0.3	KPNO
50,756.727	0.283	−23.8	0.2	KPNO
50,829.576	0.829	−20.3	0.3	KPNO
50,830.589	0.851	−19.0	0.3	KPNO
51,003.927	0.529	−25.8	0.2	KPNO
51,093.715	0.435	−25.5	0.3	KPNO
51,094.749	0.457	−25.9	0.0	KPNO
51,472.717	0.478	−26.4	−0.4	KPNO
51,731.937	0.979	−6.7	−0.4	KPNO
51,734.960	0.043	−8.5	−0.2	KPNO
51,735.940	0.064	−10.7	0.1	KPNO
51,736.881	0.084	−13.1	0.1	KPNO
51,805.823	0.547	−25.9	0.1	KPNO
52,179.745	0.482	−26.2	−0.2	KPNO
52,180.776	0.504	−26.2	−0.2	KPNO
52,182.744	0.546	−26.1	−0.1	KPNO
52,536.781	0.059	−10.4	−0.2	KPNO
52,538.784	0.102	−15.4	−0.3	KPNO

[a] McD: McDonald Observatory; KPNO: Kitt Peak National Observatory; Coravel: Haute-Provence Observatory or ESO.
[b] Velocity given zero weight.
[c] Lithium region, central wavelength 6700 Å.
[d] Hα region, central wavelength 6560 Å.

$B - V = 0.892$, G4 III), while the check star was HD 217264 (2 Psc, HR 8742; $V = 5.43$, $B - V = 0.982$, K1 III).

4. HD 37824 (V1149 ORIONIS)

4.1. *Brief History*

In an objective-prism survey of the southern sky, Bidelman & MacConnell (1973) discovered that HD 37824 ($\alpha = 5^{h}41^{m}26\overset{s}{.}8$, $\delta = 03^{\circ}46' 41''$ [J2000.0], $V = 6.7$ mag) has Ca II H and K emission lines and determined a spectral type of K1 III+F. Bopp (1984) confirmed the Ca II H and K emission and computed emission fluxes for the two lines. Hall et al. (1983) announced the discovery of the star's photometric variability and from 3 years of data found a period of 52.6 days. Lloyd Evans & Koen (1987) also detected the photometric variability of HD 37824. They found its period consistent with the orbital period given by Balona (1987), who presented the first set of orbital elements for this single-lined system. He determined a period of 53.580 days and that the orbit is nearly circular. Fekel et al. (1986) carried out a survey of chromospherically active stars. Their 11 radial velocities of HD 37824 were consistent with the

TABLE 4
PHOTOMETRIC OBSERVATIONS OF HD 37824

HJD − 2,400,000	$(V - C)_B$ (mag)	$(V - C)_V$ (mag)	$(K - C)_B$ (mag)	$(K - C)_V$ (mag)
47,417.9552	1.663	0.827	−0.325	−1.185
47,421.9485	1.673	0.817	−0.329	−1.174
47,423.9408	1.657	0.826	99.999	−1.180
47,429.9236	1.629	0.805	99.999	−1.170
47,430.9275	1.622	99.999	99.999	99.999

NOTES.—Table 4 is presented in its entirety in the electronic edition of the *Astronomical Journal*. A portion is shown here for guidance regarding its form and content.

TABLE 5
PHOTOMETRIC OBSERVATIONS OF HD 181809

HJD − 2,400,000	$(V-C)_B$ (mag)	$(V-C)_V$ (mag)	$(K-C)_B$ (mag)	$(K-C)_V$ (mag)
47,276.9450.....	0.931	1.132	−0.919	0.016
47,276.9493.....	0.921	1.130	−0.911	0.014
47,277.9423.....	0.922	1.131	−0.917	0.015
47,277.9466.....	0.922	1.126	−0.919	0.019
47,280.9578.....	0.880	1.091	−0.918	0.019

NOTES.—Table 5 is presented in its entirety in the electronic edition of the *Astronomical Journal*. A portion is shown here for guidance regarding its form and content.

orbital period of Balona (1987). An *IUE* spectrum, however, showed no evidence of the F-type secondary star suggested by Bidelman & MacConnell (1973). Hall et al. (1991) analyzed 11 years of *V*-band photometry, modeling the data with two major star spot groups.

In other wavelength regions, Morris & Mutel (1988) did not detect HD 37824 in a 5 GHz radio survey of chromospherically active stars. Dempsey et al. (1993) reported its detection as a weak, soft X-ray source with *ROSAT*, but Mitrou et al. (1997) stated that it was not a 3 σ source detection with the *EUVE* satellite.

4.2. *Orbit*

Adopting the orbital period of Balona (1987), we obtained preliminary orbital elements from our 60 radial velocities (Table 1) with BISP. One velocity had a residual greater than 3 σ, and so it was given zero weight. Then the elements were refined with SB1. Since that solution gave a very low eccentricity of 0.004 ± 0.004, a circular orbit was computed with SB1C. The tests of Lucy & Sweeney (1971) indicated that the latter solution is to be preferred. We next computed an orbital solution for the velocities of Balona (1987). Two observations on JD 2,444,235 and 2,444,639 with extremely large velocity residuals were given zero weight and the orbit recomputed. From a comparison of the variances of the eccentric-orbit solutions, the velocities of Balona (1987) were given weights of 0.05 relative to ours. In addition, 1 km s^{-1} was added to the velocities of Balona (1987) to align the zero points of the two velocity systems. The resulting circular-orbit solution of the combined data sets is given in Table 7. For a circular orbit the element *T*, a time of periastron passage, is undefined. Thus, as recommended by Batten et al. (1989), T_0, a time of maximum velocity, is listed instead. The phases of the observations and the residuals to the computed curve are given in Table 1. The observed velocities and the computed velocity curve are compared in Figure 1, in which zero phase is a time of maximum velocity.

TABLE 6
PHOTOMETRIC OBSERVATIONS OF HD 217188

HJD − 2,400,000	$(V-C)_B$ (mag)	$(V-C)_V$ (mag)	$(K-C)_B$ (mag)	$(K-C)_V$ (mag)
47,306.9800.....	99.999	99.999	99.999	−0.806
47,307.9776.....	99.999	1.161	−0.719	−0.802
47,308.9768.....	99.999	1.158	−0.716	−0.804
47,309.9727.....	1.285	1.157	−0.716	−0.802
47,310.9740.....	99.999	1.155	−0.715	−0.805

NOTES.—Table 6 is presented in its entirety in the electronic edition of the *Astronomical Journal*. A portion is shown here for guidance regarding its form and content.

TABLE 7
ORBITAL ELEMENTS OF HD 37824

Parameter	Value
P (days).....	53.57465 ± 0.00072
T_0 (HJD).....	2,448,625.022 ± 0.037
γ (km s^{-1}).....	28.117 ± 0.077
K (km s^{-1}).....	26.49 ± 0.11
e.....	0.0 adopted
$a \sin i$ (km).....	$19.518 \pm 0.083 \times 10^6$
$f(m)$ ($M_\odot$).....	0.1035 ± 0.0013
Standard error of an observation of unit weight (km s^{-1}).....	0.6

4.3. *Spectral Type and Abundance*

Strassmeier & Fekel (1990) identified several luminosity-sensitive and temperature-sensitive line ratios in the 6430–6465 Å region. Those critical line ratios and the general appearance of the spectrum were employed as spectral-type criteria. The spectra of HD 37824 were compared with those of late-G and early-K giants from the lists of Keenan & McNeil (1989) and Fekel (1997), obtained at KPNO with the same telescope, spectrograph, and detector as our spectra of HD 37824. To facilitate a comparison, the spectra of the reference stars were rotationally broadened and shifted in radial velocity with a computer program developed by Huenemoerder & Barden (1984) and Barden (1985). The 6430 Å region of HD 37824 is fitted best by the spectrum of β Gem, which has a spectral type of K0 III (Keenan & McNeil 1989) and a mean $[\mathrm{Fe/H}] = -0.0$ (Taylor 1999). Therefore, we classify HD 37824 as a K0 III star and conclude that it has a solar [Fe/H] value. Our spectral type is in good agreement with the K1 III and K0 III classifications of Bidelman & MacConnell (1973) and Houk & Swift (1999), respectively.

Our estimated metal abundance from the spectrum comparison is similar to the value of −0.1 of Fekel & Balachandran (1994). However, it differs from that of Randich et al. (1993), who determined $[\mathrm{Fe/H}] = -0.5$. Recently, Morel et al. (2003) have determined abundances for six single-lined chromospherically active binaries, five of which were analyzed previously by Randich et al. (1993, 1994). For four of the five systems,

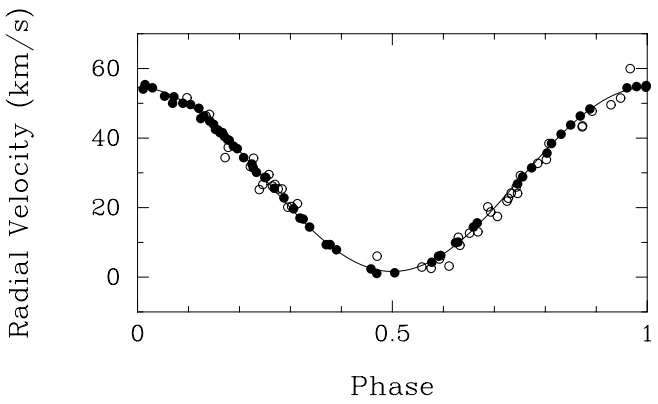

FIG. 1.—Computed radial velocity curve of HD 37824 compared with the observations of velocity from SAAO (*open circles*) and from McDonald Observatory and KPNO (*filled circles*). Two SAAO velocities given zero weight because of very large residuals have not been plotted. Zero phase is a time of maximum velocity.

TABLE 8
FUNDAMENTAL PROPERTIES OF HD 37824

Parameter	Value	Reference
V (mag)	6.59	1
$B - V$ (mag)	1.14	1
π (arcsec)	0.00693 ± 0.00113	2
Spectral type	K0 III	1
$v \sin i$ (km s^{-1})	14.9 ± 1.0	3
M_V (mag)	0.68 ± 0.37	1
L ($L_\odot$)	67 ± 23	1
R ($R_\odot$)	12.6 ± 2.2	1

REFERENCES.—(1) This paper; (2) Perryman 1997; (3) Fekel 1997.

Morel et al. (2003) found substantially larger iron abundances than those determined by Randich et al. (1993, 1994). Thus, we conclude that HD 37824 has an iron abundance that is essentially solar.

4.4. *Basic Properties*

We searched the literature and examined our own data for the brightest known visual magnitude and corresponding $B - V$ of HD 37824. From the APT data of Strassmeier et al. (1989), HD 37824 was brightest in 1985, with a differential V magnitude of 0.50. To convert this to an apparent V magnitude, we adopted $V = 6.09$ (Perryman 1997) for the comparison star, HD 38309. This resulted in a maximum V magnitude of 6.59. O'Neal et al. (1996) showed that on some heavily spotted stars the observed maximum V magnitude underestimates the brightness of the unspotted star by 0.3–0.4 mag. Nevertheless, we have adopted the historical maximum as the unspotted V magnitude of the primary since for HD 37824 we are unable to determine a specific correction. This magnitude, combined with the *Hipparcos* parallax of 0.″00693 ± 0.″00113 (Perryman 1997), resulted in $M_v = 0.68 \pm 0.37$ mag. HD 37824 is only 14° below the Galactic plane, and so at a distance of 144 ± 24 pc it may be affected by a modest amount of interstellar extinction. Thus, we have adopted the mean extinction value of Henry et al. (2000) for the absolute magnitude calculation. As a result of that correction, the $B - V$ color index of 1.14 mag from our APT data becomes $(B - V)_0 = 1.10$ mag. This value was used in conjunction with Table 3 of Flower (1996) to obtain a bolometric correction and effective temperature. These values were used to compute a luminosity $L = 67 \pm 23\ L_\odot$ and a radius $R = 12.6 \pm 2.2\ R_\odot$. The uncertainties in the computed quantities are dominated by the uncertainty in the parallax and to a lesser extent in the effective temperature, with the latter uncertainty estimated to be ±100 K. If the unspotted V magnitude were 0.2 mag brighter than our adopted value, the luminosity would be increased by 20% and the radius by 10%. The various quantities are summarized in Table 8.

The minimum radius of the giant, computed from $v \sin i = 15$ km s^{-1} (Fekel 1997) and a mean rotation period of 53.12 days (§ 4.5), is 15.7 ± 1.0 $R_\odot$, somewhat larger than the radius of 12.6 ± 2.2 $R_\odot$ determined from its *Hipparcos* parallax. Such a radius discrepancy has been found for a few other chromospherically active giants, and Fekel et al. (1999) discussed possible sources of the problem.

4.5. *Photometric Analysis*

The $V - C$ differential magnitudes in the V passband from Table 4 are plotted against Julian date in Figure 2. The top panel displays all 15 observing seasons; the second through fifth panels show selected individual seasons on expanded time axes. We performed separate periodogram analyses for each observing season on both the V and B observations. The resulting periods, which we take to be individual measures of the stellar rotation period, are given in column (6) of Table 9 along with the Julian date range of each observing season (col. [3]), the number of observations in each season (col. [4]), the seasonal mean $V - C$ differential magnitude (col. [5]), the photometric amplitude (col. [7]), the seasonal mean $K - C$ differential magnitude (col. [8]), and the standard deviation of the $K - C$ differential magnitudes within each season (col. [9]). The photometric amplitudes were estimated from the light curves; the cited values refer to the cycles with the largest amplitude within each observing season. The largest amplitudes for the whole 15 year data set (0.27 and 0.31 mag in V and B, respectively) occurred in the tenth season.

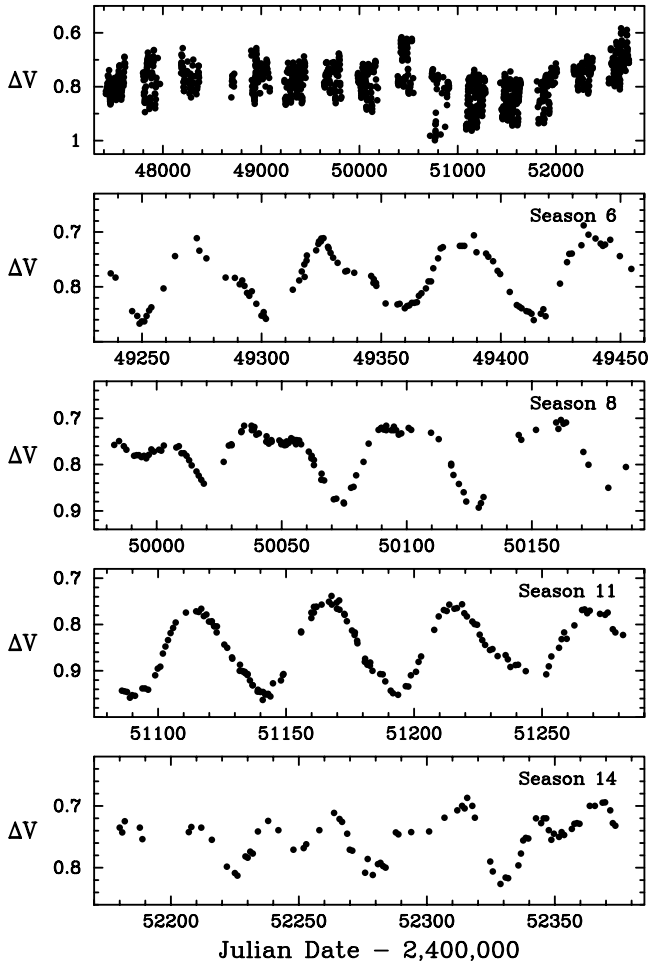

FIG. 2.—Variable minus comparison differential magnitudes of HD 37824 in V from the 0.4 m APT plotted against Julian date. The top panel shows all 15 years of data, while the remaining panels show selected individual observing seasons.

The standard deviations of the $K - C$ differential magnitudes indicate that both the check and comparison stars are constant from night to night to approximately the limit of our photometric precision with this telescope. The $K - C$ seasonal means, however, probably vary over a range of several millimags. These means are plotted in Figure 3 (*bottom*) to the same scale as the $V - C$ seasonal means shown in Figure 3 (*top*). While we cannot be sure whether the slight variation in the $K - C$ means arises from the comparison star or the check star, the amplitude

TABLE 9

RESULTS FROM PHOTOMETRIC ANALYSIS OF HD 37824

Season (1)	Photometric Band (2)	HJD Range (HJD − 2,400,000) (3)	N_{obs} (4)	$\langle V - C \rangle$ (mag) (5)	Photometric Period (days) (6)	Peak-to-Peak Amplitude (mag) (7)	$\langle K - C \rangle$ (mag) (8)	σ_{K-C} (mag) (9)
1	*V*	47,417–47,615	112	0.7986	55.67 ± 0.75	0.15	−1.1767	0.0109
1	*B*	47,417–47,623	127	1.6340	55.79 ± 0.72	0.18	−0.3322	0.0120
2	*V*	47,796–47,971	71	0.7735	55.41 ± 0.83	0.20	−1.1754	0.0122
2	*B*	47,789–47,973	97	1.6287	55.30 ± 0.73	0.20	−0.3295	0.0117
3	*V*	48,185–48,368	61	0.7607	56.42 ± 1.26	0.16	−1.1740	0.0108
3	*B*	48,183–48,365	58	1.5802	56.41 ± 0.77	0.16	−0.3397	0.0205
4	*V*	48,696–48,725	9	0.7814	...	...	−1.1777	0.0101
4	*B*	48,696–48,725	7	1.6067	...	...	−0.3533	0.0033
5	*V*	48,899–49,088	77	0.7581	55.35 ± 0.78	0.19	−1.1713	0.0070
5	*B*	48,899–49,088	76	1.5798	55.65 ± 0.74	0.21	−0.3459	0.0072
6	*V*	49,236–49,454	107	0.7832	54.70 ± 0.28	0.15	−1.1794	0.0060
6	*B*	49,236–49,454	111	1.6052	54.66 ± 0.34	0.16	−0.3450	0.0065
7	*V*	49,638–49,815	78	0.7688	57.60 ± 0.79	0.17	−1.1801	0.0059
7	*B*	49,638–49,815	77	1.5883	58.06 ± 0.89	0.21	−0.3425	0.0058
8	*V*	49,982–50,187	115	0.7713	57.29 ± 0.91	0.18	−1.1805	0.0055
8	*B*	49,982–50,187	119	1.5874	57.08 ± 1.12	0.19	−0.3447	0.0052
9	*V*	50,391–50,548	75	0.7230	52.52 ± 0.40	0.20	−1.1780	0.0073
9	*B*	50,391–50,548	75	1.5302	52.49 ± 0.39	0.24	−0.3429	0.0065
10	*V*	50,718–50,911	44	0.8316	53.07 ± 0.40	0.27	−1.1797	0.0071
10	*B*	50,718–50,911	46	1.6540	52.99 ± 0.42	0.31	−0.3468	0.0082
11	*V*	51,085–51,281	147	0.8512	51.38 ± 0.16	0.21	−1.1735	0.0081
11	*B*	51,085–51,280	148	1.6794	51.50 ± 0.15	0.24	−0.3389	0.0079
12	*V*	51,434–51,640	122	0.8519	51.50 ± 0.21	0.18	−1.1717	0.0063
12	*B*	51,434–51,646	119	1.6842	51.32 ± 0.20	0.20	−0.3378	0.0068
13	*V*	51,805–52,007	72	0.8116	50.05 ± 0.42	0.17	−1.1720	0.0062
13	*B*	51,805–52,008	77	1.6340	49.81 ± 0.40	0.19	−0.3420	0.0066
14	*V*	52,180–52,373	78	0.7502	55.28 ± 0.93	0.13	−1.1736	0.0060
14	*B*	52,180–52,373	78	1.5708	55.32 ± 0.85	0.15	−0.3421	0.0088
15	*V*	52,538–52,741	103	0.7093	52.54 ± 0.64	0.21	−1.1721	0.0056
15	*B*	52,538–52,740	102	1.5278	52.36 ± 0.63	0.27	−0.3418	0.0071

is much smaller than the observed 0.14 mag long-term variations in the $V - C$ differential magnitudes and so has no significant effect on our analysis of HD 37824.

The long-term changes in mean brightness seen in Figure 3 (*top*) indicate significant changes in the average filling factor of spots on the photosphere of HD 37824 but with no obvious periodicity. Similarly, the second and third panels of Figure 3 document year-to-year variations in the photometric amplitude and period of the star but again without obvious periodicity. The plotted periods are the means of the two periods derived separately for each season from the *B* and *V* observations. If HD 37824 has an activity cycle analogous to the sunspot cycle in our own Sun, we might expect changes in the observed rotation period due to a combination of the star's differential rotation and systematic changes in the spot latitudes as the cycle progresses. However, as seen in the top two panels of Figure 4, these period changes show no correlation with the seasonal mean brightness or with the amplitude of the light curve and so do not appear to be tied to the level of spottedness of the star. Furthermore, the third panel of Figure 4 shows no correlation between the amplitude and the mean brightness, indicating that rotational modulation of spot visibility is largely independent of the mean level of spottedness.

We estimated times of photometric minimum by inspection of the light curves and converted these times of minimum to orbital phases using the orbital period determined in § 4.2 and a time of superior conjunction of the K0 III primary. Many of the light curves reveal two separate minima within a single rotation cycle (Fig. 2), indicating relatively large spot regions on opposite hemispheres of the star. The orbital phases of the times of minimum are plotted in Figure 4 (*bottom*), in which the phases of the deeper and shallower minima within a given observing season are plotted as filled and open circles, respectively. Clear migration of the spots to smaller orbital phases demonstrates that HD 37824 is rotating slightly faster than synchronous. The phases of minimum lie along two straight line segments, suggesting two long-lived spot regions separated by 0.5 phase units. Spot A is visible throughout the 15 year span of our observations, although it is sometimes the smaller of the two spot regions. Spot B faded from visibility as a separate photometric minimum for 4 years but reappeared along an extension of the original trend in the migration curve. The times of minimum for spot A fit the linear trend with an rms dispersion of only 3.9 days; the rms of spot B is only 2.4 days. The slopes of spot A and spot B give mean rotation periods of 53.09 ± 0.02 and 53.15 ± 0.01 days, respectively, and are identical within their uncertainties. We take the mean of the two periods, 53.12 ± 0.01 days, as our best determination of the rotation period of the star, which, compared with the orbital period of 53.5746 days, gives a measured rotation rate 0.8% faster than synchronous rotation.

It appears that spot activity on the photosphere of HD 37824 has been dominated for 15 years by two long-lived active regions on opposite hemispheres of the star. The small rms fit of the times of minimum to the linear trends in the migration curve and the agreement in the slopes of the two spot curves indicate

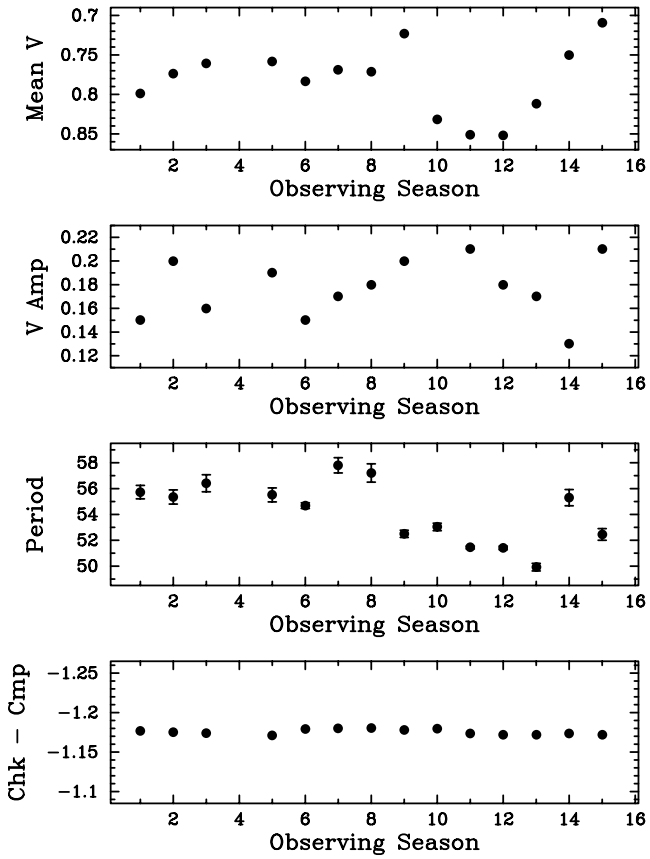

FIG. 3.—HD 37824 yearly mean differential V magnitudes (*first panel*), V amplitudes (*second panel*), photometric periods (*third panel*), and check minus comparison yearly mean differential V magnitudes (*fourth panel*), all from Table 9, plotted for each of the 15 observing seasons.

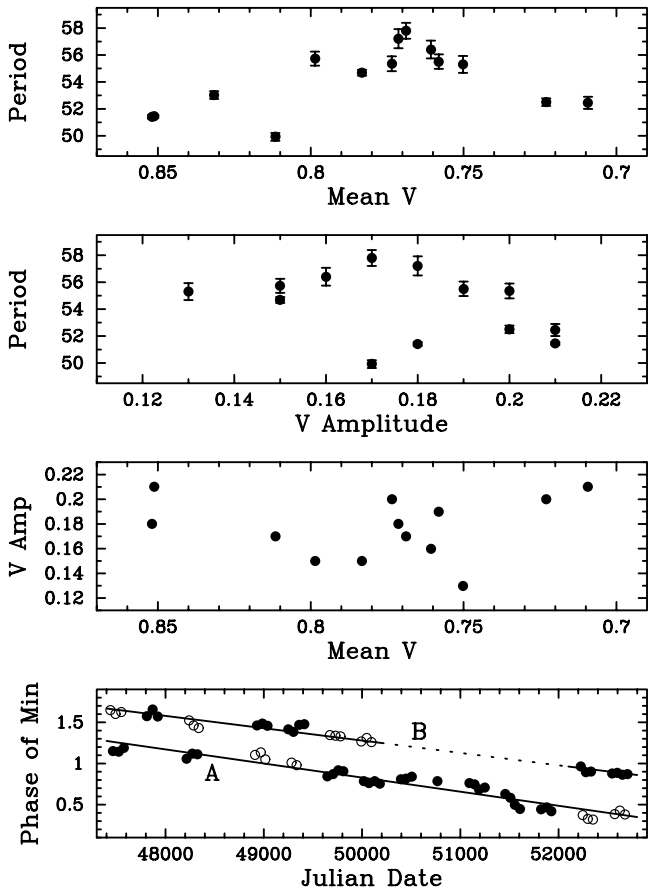

FIG. 4.—HD 37824 seasonal photometric periods plotted against yearly mean V brightness (*first panel*) and V amplitude (*second panel*), V amplitude plotted against mean brightness (*third panel*), and phases of spot minimum plotted against Julian date (*fourth panel*). No significant correlations are observed in the top three panels. The bottom panel suggests that two spotted regions persisted on HD 37824 for 15 years.

that all of our photometry is consistent with a single rotation period of 53.12 days. Therefore, our measured rotation periods from the individual seasons probably have true errors larger than the formal uncertainties in the period analysis. As discussed by Fekel et al. (2002), the observed photometric periods in chromospherically active stars must be interpreted with care, since they can be affected by the growth and decay of individual spots at various longitudes, as well as the formation of new and decay of old clumps of spots by differential rotation, so that the photometric period at any epoch may not correspond precisely to the rotation period of *any* stellar latitude. It appears, therefore, that our photometry does not successfully reveal any differential rotation in HD 37824.

5. HD 181809 (V4138 SAGITTARII)

5.1. *Brief History*

Bidelman & MacConnell (1973) discovered the Ca II H and K emission lines of HD 181809 ($\alpha = 19^{h}22^{m}40\overset{s}{.}3$, $\delta = -20^{\circ}38'34''$ [J2000.0], $V = 6.5$ mag) in the same objective-prism survey that produced the chromospherically active star HD 37824. They classified HD 181809 as K1 III+F, while Houk & Smith-Moore (1988) called it K2 IIIp and noted that its CN strength was similar to that of a dwarf star. Lloyd Evans & Koen (1987) carried out a photometric survey of the chromospherically active stars discovered by Bidelman & MacConnell (1973) and found HD 181809 to have a V magnitude variation of about 0.26 mag with a period of 59 days. This period is quite different from the orbital period of 13.048 days determined by Balona (1987). For HD 181809 Hooten & Hall (1990) analyzed five groups of photometry ranging over about 11 years. They determined a "best" period of 60.23 days and found that, during the time covered by their observations, HD 181809 had a maximum V magnitude amplitude of 0.3 mag.

Slee et al. (1987) included HD 181809 in a microwave survey of southern, active stars. At 8.4 GHz they detected emission on only three of 22 nights. Dempsey et al. (1993) reported it to be a weak, soft X-ray source with *ROSAT*. However, Mitrou et al. (1997) stated that, like HD 37824, HD 181809 was not detected as a 3 σ source by the *EUVE* satellite.

5.2. *Spectroscopic Orbit*

The orbital period of Balona (1987) was initially adopted, and preliminary orbital elements were determined with BISP from our 54 radial velocities in Table 2. These elements were refined by obtaining a solution with the SB1 program. The velocities on JD 2,444,180 and 2,444,894 had residuals greater than 3 σ, so they were given zero weight, and another solution was computed. Then, separate orbital solutions were determined for the velocities given by Balona (1987) and Collier Cameron (1987). The variances of those two solutions were compared with that of our velocities. Appropriate weights and zero-point velocity offsets were applied to the velocities given by Balona (1987) and Collier Cameron (1987). When combined with our data, the two sets of velocities did not significantly improve the element

TABLE 10
ORBITAL ELEMENTS OF HD 181809

Parameter	Value
P (days)	13.046773 ± 0.000064
T (HJD)	2,449,248.005 ± 0.273
γ (km s^{-1})	−13.872 ± 0.037
K (km s^{-1})	9.887 ± 0.054
e	0.0403 ± 0.0053
ω (deg)	52.8 ± 7.5
$a \sin i$ (km)	1.7723 ± 0.0097 × 10^6
$f(m)$ ($M_\odot$)	0.001306 ± 0.000021
Standard error of an observation of unit weight (km s^{-1})	0.3

uncertainties. The orbital solution of our velocities only, with two given zero weight, has a low eccentricity of 0.040 ± 0.005. Thus, we computed a circular orbit with SB1C. The tests of Lucy & Sweeney (1971) indicated that the eccentric-orbit solution is to be preferred, and so it is listed in Table 10. The observed unit-weight velocities and the computed velocity curve are compared in Figure 5, in which zero phase is a time of periastron passage.

5.3. *Spectral Type and Abundance*

Following the classification method used for HD 37824, we compared the spectrum of HD 181809 in the 6430 Å region with that of various G and K subgiants and giants. The spectrum of HD 181809 appears to be intermediate between δ Eri (K0 IV; Keenan & McNeil 1989) and β Gem (K0 III; Keenan & McNeil 1989). Thus, we classify it as K0 III–IV. This is slightly earlier and less luminous than the K1 III and K2 III classifications of Bidelman & MacConnell (1973) and Houk & Smith-Moore (1988), respectively. From the mean abundances of our reference stars (Taylor 1999), we estimate an [Fe/H] value that is slightly less than solar. This is in reasonable agreement with determinations by Fekel & Balachandran (1994), Morel et al. (2004), and Randich et al. (1993), who found [Fe/H] = 0.0, −0.09, and −0.3, respectively.

5.4. *Basic Properties*

We searched the literature and examined our own data for the brightest known visual magnitude and corresponding $B - V$ of HD 181809. From the APT data in Figure 6 (§ 5.5), HD 181809 is currently at its brightest, with a differential V magnitude of 0.93. To convert this to an apparent V magnitude, we adopted $V = 5.57$ (Perryman 1997) for our comparison star, HD 182629. This resulted in a magnitude at maximum of $V = 6.50$ mag. We have adopted this historical maximum as the unspotted V magnitude of the primary. This magnitude, combined with the *Hipparcos* parallax (Perryman 1997), corresponding to a distance of 88 ± 7 pc, resulted in $M_v = 1.78 \pm 0.16$ mag. Although HD 181809 is only 16° below the Galactic plane, we assumed no interstellar reddening because it is less than 100 pc from the Sun. A $B - V$ color index of 1.00 mag from our APT data was used in conjunction with Table 3 of Flower (1996) to obtain a bolometric correction and effective temperature. These values were then combined to produce a luminosity $L = 21.1 \pm 3.1\ L_\odot$ and a radius $R = 6.5 \pm 0.6\ R_\odot$. The uncertainties in the computed quantities are dominated by the parallax and effective temperature uncertainties. A brighter adopted unspotted V magnitude would result in luminosity and radius increases similar to those found for HD 37824. The various quantities are summarized in Table 11.

By comparing the giant's minimum radius, computed from $v \sin i = 4$ km s^{-1} (Fekel 1997) and a mean rotation period of 59.85 days (§ 5.5), with the radius determined from its *Hipparcos* parallax, a rotational inclination of 46^{+20}_{-14} deg is found for the primary.

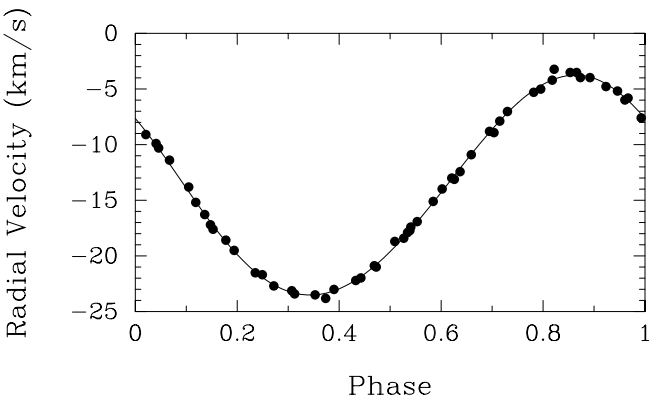

FIG. 5.—Computed radial velocity curve of HD 181809 compared with the observations. Two velocities given zero weight have not been plotted. Zero phase is a time of maximum velocity.

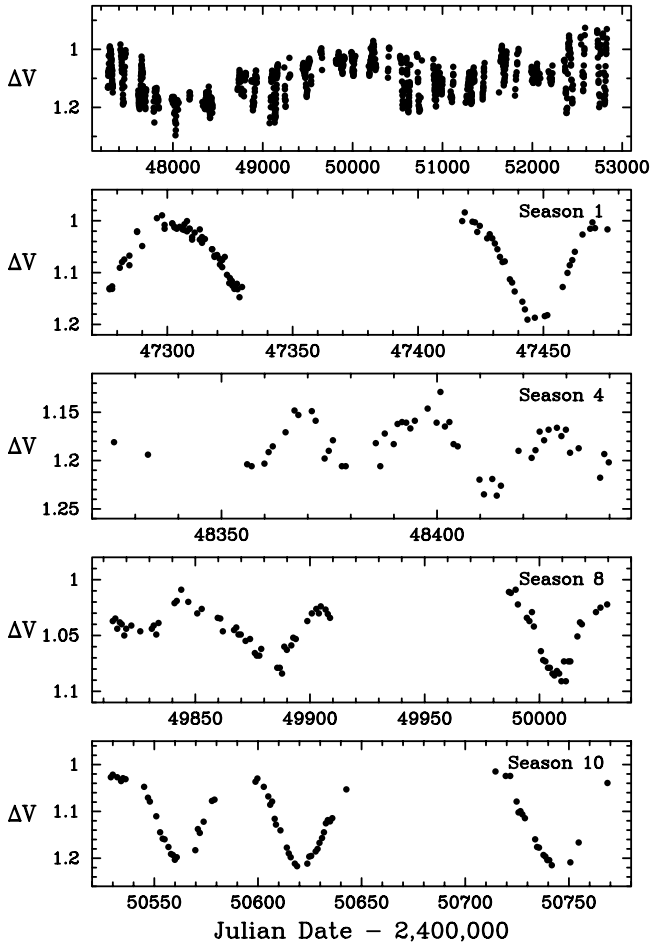

FIG. 6.—Variable minus comparison differential magnitudes of HD 181809 in V from the 0.4 m APT plotted against Julian date. The top panel shows all 16 years of data, while the remaining panels show selected individual observing seasons.

TABLE 11
FUNDAMENTAL PROPERTIES OF HD 181809

Parameter	Value	Reference
V (mag)	6.50	1
$B - V$ (mag)	1.00	1
π (arcsec)	0.01140 ± 0.00085	2
Spectral type	K0 III–IV	1
$v \sin i$ (km s^{-1})	4.2 ± 1.0	3
M_V (mag)	1.78 ± 0.19	1
L ($L_\odot$)	21.8 ± 3.8	1
R ($R_\odot$)	6.7 ± 0.6	1

REFERENCES.—(1) This paper; (2) Perryman 1997; (3) Fekel 1997.

5.5. *Photometric Analysis*

The $V - C$ differential magnitudes in the V passband from Table 5 are plotted against Julian date in Figure 6. As in Figure 2, the top panel displays the entire data set, while the remaining panels show selected individual seasons. The results of our periodogram analyses for each season are given in Table 12 in the same format as for Table 9. The largest amplitude (0.26 and 0.29 mag in V and B, respectively) occurred in the most recent observing season.

The standard deviations of the $K - C$ differential magnitudes average 0.0081 and 0.0089 mag in V and B, respectively, for observing seasons 5–16 since we converted to the precision photometer. They are slightly larger than our nominal data precision because HD 181809 lies at a declination of -21° and so is observed through a greater air mass than most of our targets. The standard deviations of the seasonal means of the $K - C$ magnitudes are 0.0022 and 0.0039 mag in V and B, respectively, so we find little or no variability in either the comparison or check star on day-to-day and year-to-year timescales. The seasonal means in V are plotted in Figure 7 (*bottom*).

Long-term changes in the mean brightness of HD 181809 with a range of 0.16 mag in V are seen in Figure 7 (*top*), indicating changes in the spot filling factor on a timescale of years. Similarly, the second and third panels show variations in the photometric amplitude and period of the star, respectively, on a timescale of several years. In particular, the third panel suggests a possible 6 yr variation. As is the case for HD 37824, the top three panels of Figure 8 do not demonstrate significant correlations between the photometric period, mean brightness, and amplitude.

The weighted mean of our seasonal photometric periods is 60.0 ± 0.1 days. Times of photometric minimum derived by inspection of the light curves and converted to photometric

TABLE 12
RESULTS FROM PHOTOMETRIC ANALYSIS OF HD 181809

Season (1)	Photometric Band (2)	HJD Range (HJD − 2,400,000) (3)	N_{obs} (4)	$\langle V - C \rangle$ (mag) (5)	Photometric Period (days) (6)	Peak-to-Peak Amplitude (mag) (7)	$\langle K - C \rangle$ (mag) (8)	σ_{K-C} (mag) (9)
1	V	47,276–47,475	92	1.0649	58.13 ± 0.31	0.19	0.0140	0.0087
1	B	47,276–47,475	91	0.8531	58.25 ± 0.33	0.22	−0.9125	0.0109
2	V	47,615–47,844	106	1.1511	52.72 ± 0.88	0.16	0.0112	0.0106
2	B	47,616–47,841	109	0.9512	51.75 ± 0.98	0.18	−0.9151	0.0113
3	V	47,987–48,192	33	1.1942	62.93 ± 1.70	0.13	0.0160	0.0126
3	B	47,987–48,192	30	0.9983	63.24 ± 2.01	0.15	−0.9161	0.0098
4	V	48,325–48,439	52	1.1833	58.88 ± 1.88[a]	0.09	0.0098	0.0138
4	B	48,325–48,439	53	0.9928	60.02 ± 1.36[a]	0.09	−0.9078	0.0115
5	V	48,721–48,934	58	1.1234	60.51 ± 0.34	0.12	0.0152	0.0089
5	B	48,721–48,934	54	0.9165	61.05 ± 0.39	0.15	−0.9438	0.0083
6	V	49,078–49,301	70	1.1397	62.01 ± 0.40	0.14	0.0199	0.0079
6	B	49,078–49,301	75	0.9318	62.09 ± 0.46	0.18	−0.9339	0.0112
7	V	49,443–49,662	53	1.0707	65.32 ± 0.79	0.11	0.0236	0.0060
7	B	49,443–49,662	53	0.8533	64.98 ± 0.80	0.12	−0.9332	0.0085
8	V	49,814–50,029	76	1.0476	63.21 ± 1.19	0.08	0.0200	0.0074
8	B	49,812–50,029	81	0.8309	64.27 ± 1.17	0.09	−0.9336	0.0071
9	V	50,181–50,406	54	1.0342	64.47 ± 0.79	0.11	0.0185	0.0080
9	B	50,181–50,406	60	0.8131	65.25 ± 0.77	0.15	−0.9329	0.0100
10	V	50,529–50,768	70	1.1263	60.04 ± 0.23	0.19	0.0197	0.0081
10	B	50,527–50,768	74	0.9262	59.86 ± 0.22	0.21	−0.9323	0.0080
11	V	50,897–51,122	70	1.1245	58.94 ± 0.28	0.18	0.0175	0.0067
11	B	50,897–51,126	73	0.9266	59.03 ± 0.28	0.18	−0.9356	0.0072
12	V	51,259–51,465	70	1.1214	58.13 ± 0.67	0.11	0.0189	0.0104
12	B	51,259–51,465	76	0.9176	57.89 ± 0.70	0.15	−0.9317	0.0100
13	V	51,629–51,847	46	1.0546	60.99 ± 0.58	0.14	0.0175	0.0097
13	B	51,629–51,847	48	0.8365	61.40 ± 0.57	0.17	−0.9314	0.0093
14	V	51,990–52,225	54	1.0888	63.14 ± 0.93	0.07	0.0197	0.0077
14	B	51,990–52,225	52	0.8800	62.99 ± 1.16	0.08	−0.9307	0.0097
15	V	52,355–52,584	63	1.0713	60.28 ± 0.46	0.26	0.0221	0.0083
15	B	52,355–52,584	66	0.8642	60.84 ± 0.47	0.28	−0.9287	0.0091
16	V	52,721–52,828	45	1.0608	59.62 ± 0.60	0.26	0.0182	0.0092
16	B	52,720–52,828	45	0.8435	59.44 ± 0.64	0.29	−0.9285	0.0082

[a] Observed photometric period multiplied by 2, since star had significant spot activity on opposite hemispheres.

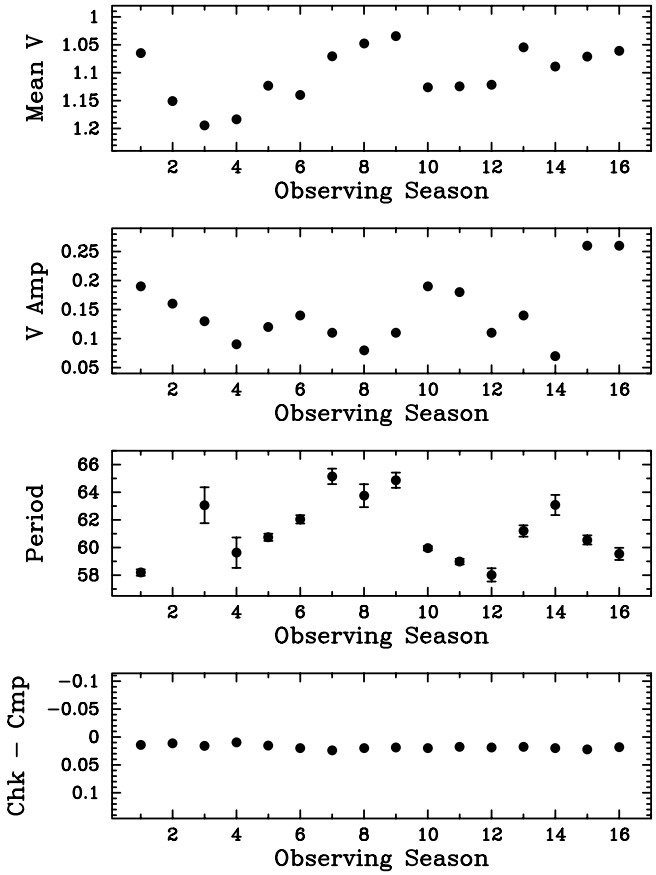

FIG. 7.—HD 181809 yearly mean differential V magnitudes (*first panel*), V amplitudes (*second panel*), photometric periods (*third panel*), and check minus comparison yearly mean differential V magnitudes (*fourth panel*), all from Table 12, plotted for each of the 16 observing seasons.

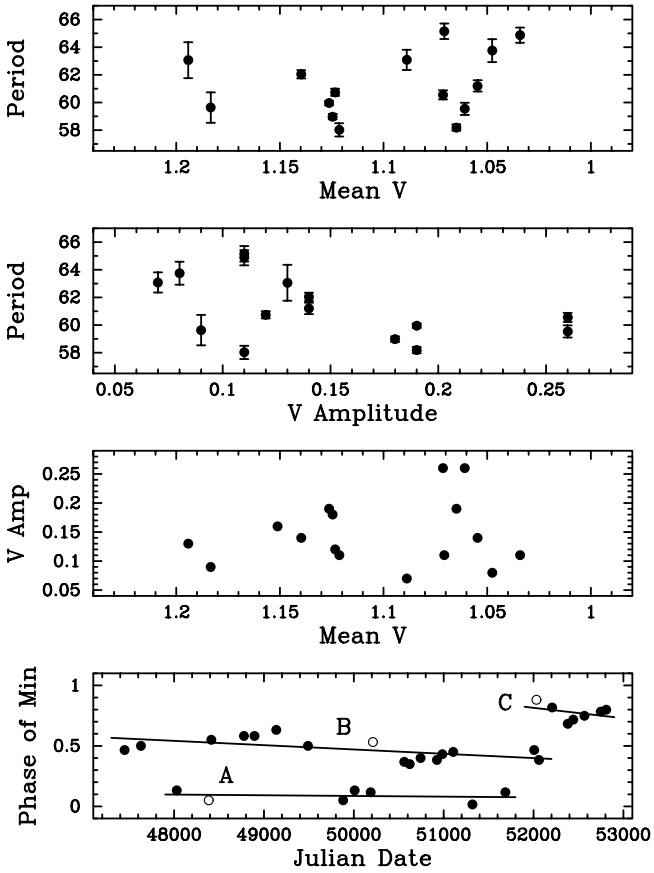

FIG. 8.—HD 181809 seasonal photometric periods plotted against yearly mean V brightness (*first panel*) and V amplitude (*second panel*), V amplitude plotted against mean brightness (*third panel*), and phases of spot minimum plotted against Julian date (*fourth panel*). No significant correlations are observed in the top three panels. The bottom panel suggests at least one long-lived spotted region on HD 181809.

phases with the mean 60.0 rotation period and an arbitrary epoch are plotted in Figure 8 (*bottom*). In most cases, only a single photometric minimum was evident in each rotation cycle, but occasional secondary minima were observed and are plotted as open circles. Little, if any, migration of the spots in phase is seen, since the phases were computed with the mean rotation period. Most of the phases of minimum lie closely along two straight line segments, which we identify as spots A and B in the figure. Near the end of our photometric record, the minimum associated with spot A disappears and is replaced by a new minimum at a third rotational phase, which we designate as spot C. Least-squares line fits to the phases of spots A, B, and C give rotation periods of 59.98, 59.87, and 59.69 days, respectively, with a mean of 59.85 days, which we take as our best value for HD 181809's rotation period. Therefore, the star is rotating much slower than synchronous rotation with the 13 day orbital period. The range of the three periods, $\Delta P/P$, is only 0.48%, and the times of minimum for spots A, B, and C fit the linear trends with rms dispersions of only 3.1, 4.3, and 4.1 days, respectively.

Like HD 37824, spot activity on HD 181809 appears to be concentrated near two stellar longitudes for most of the time span of our observations. The low $\Delta P/P$ of the three spot periods implies that the much larger spread in our seasonal photometric periods in Table 12 is probably not the result of differential rotation but is likely to be caused by the complicating effects of the growth and decay of spots at various longitudes within individual observing seasons. In addition, the small number of photometric cycles in a single observing season, combined with the continually evolving light curve, makes it difficult to measure the rotation period accurately within a single season. As is the case for HD 37824, we see little differential rotation in HD 181809.

6. HD 217188 (AZ PISCIUM)

6.1. *Brief History*

Bidelman (1981) reported the discovery of moderate Ca II H and K emission in the K giant star HD 217188 ($\alpha = 22^{\rm h}58^{\rm m}52\overset{\rm s}{.}9$, $\delta = -00^\circ 18' 57''$ [J2000.0], $V = 7.4$ mag). Following its identification as a chromospherically active star, Boyd et al. (1985) found light variations with a V amplitude of 0.18 mag and estimated a period of 84.4 days. Strassmeier et al. (1989) obtained additional photometric data and determined a period of 91.2 days. Six radial velocities given by Fekel et al. (1986) showed a velocity variation of 9 km s^{-1}. Additional velocities resulted in a preliminary orbit, given in Strassmeier et al. (1993), with a period of 47.121 days and an eccentricity of 0.50. More recently, De Medeiros & Udry (1999) computed an orbit with numerous Coravel velocities. They found slightly smaller values of the period and eccentricity.

Helfand et al. (1999) carried out a radio survey at 20 cm and detected a number of chromospherically active stars, including HD 217188. The star was also seen by *ROSAT* as a weak X-ray

TABLE 13
ORBITAL ELEMENTS OF HD 217188

Parameter	Value
P (days)	47.12087 ± 0.00069
T (HJD)	2,448,622.951 ± 0.065
γ (km s^{-1})	−20.554 ± 0.038
K (km s^{-1})	10.347 ± 0.055
e	0.4703 ± 0.0041
ω (deg)	358.65 ± 0.74
$a \sin i$ (km)	5.917 ± 0.035 × 10^6
$f(m)$ ($M_\odot$)	0.003726 ± 0.000066
Standard error of an observation of unit weight (km s^{-1})	0.3

source in the hard spectral band between 0.5 and 2.0 keV (Schwope et al. 2000).

6.2. *Spectroscopic Orbit*

The orbital elements of De Medeiros & Udry (1999) were adopted as starting values. With the SB1 program we obtained an orbital solution of our 52 McDonald and KPNO velocities from Table 3. The velocity on JD 2,445,358 had a residual that was greater than 3 σ, and so it was given zero weight, and the orbit was recomputed. An orbital solution was next obtained with the 31 Coravel velocities. From a comparison of the variances of the two solutions, the Coravel velocities were given weights of 1.0 relative to our velocities. Since the center-of-mass velocities of the two solutions were essentially identical, a solution of the combined data sets was obtained. We list the orbital elements of this final solution in Table 13. The Coravel velocities are given along with ours in Table 3. The observed velocities and the computed velocity curve are compared in Figure 9, in which zero phase is a time of periastron passage.

6.3. *Spectral Type and Abundance*

We compared the spectrum of HD 217188 in the 6430 Å region with that of various G and K giants. The spectrum of HD 217188 is most similar to that of β Gem. Thus, we classify it as a K0 III and conclude that its [Fe/H] abundance is essentially solar. Our spectral type is in agreement with that given by Bidelman (1981) and Houk & Swift (1999), while our estimated iron abundance is in accord with [Fe/H] = 0.0 found by Fekel & Balachandran (1994) and [Fe/H] = −0.16 determined by Morel et al. (2004).

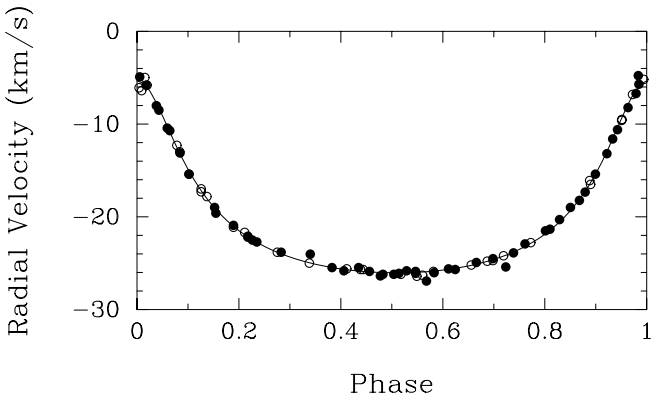

FIG. 9.—Computed radial velocity curve of HD 217188 compared with the observations. Filled circles show McDonald and KPNO velocities, and open circles show Coravel velocities. Zero phase is a time of periastron passage.

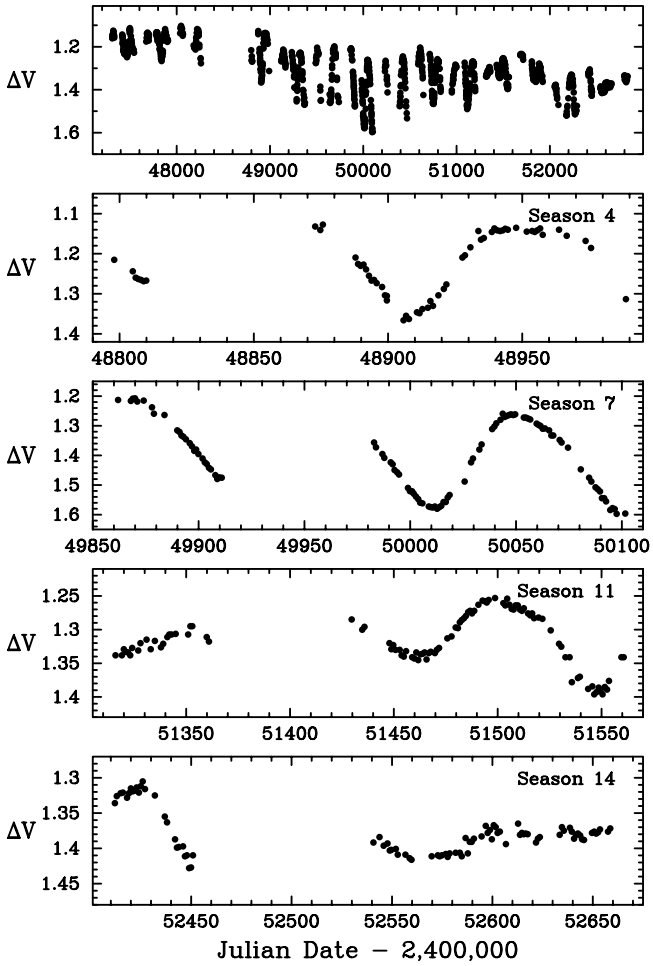

FIG. 10.—Variable minus comparison differential magnitudes of HD 217188 in V from the 0.4 m APT plotted against Julian date. The top panel shows all 15 years of data, while the remaining panels show selected individual observing seasons.

6.4. *Basic Properties*

We searched the literature and examined our own data for the brightest known visual magnitude and corresponding $B - V$ of HD 217188. From the APT data in Figure 10 (§ 6.5), HD 217188 was brightest in our first season of observation, with a differential V magnitude of 1.10. To convert this to an apparent V magnitude, we assumed $V = 6.22$ (Perryman 1997) for our comparison star, HD 217428. This resulted in a magnitude at maximum of $V = 7.32$, which we have adopted as the unspotted V magnitude of the primary. This magnitude, combined with the *Hipparcos* parallax of 0.″00678 ± 0.″00088 (Perryman 1997), which corresponds to a distance of 148 ± 20 pc, resulted in $M_v = 1.48 \pm 0.28$ mag. Since HD 217188 is 52° below the Galactic plane, we have assumed no interstellar reddening. A $B - V$ color index of 1.01 mag from our APT data was used in conjunction with Table 3 of Flower (1996) to obtain a bolometric correction and effective temperature. These values were used to compute a luminosity $L = 28.3 \pm 7.3\ L_\odot$ and a radius $R = 7.6 \pm 1.0\ R_\odot$. The uncertainties in the computed quantities are dominated by the uncertainty in the parallax and to a lesser extent in the effective temperature. A brighter adopted unspotted V magnitude would result in luminosity and radius increases similar to those found for HD 37824. The various quantities are summarized in Table 14.

By comparing the giant's minimum radius, computed from $v \sin i = 4$ km s^{-1} (Fekel 1997) and a mean rotation period of

TABLE 14
FUNDAMENTAL PROPERTIES OF HD 217188

Parameter	Value	Reference
V (mag)	7.32	1
$B - V$ (mag)	1.01	1
π (arcsec)	0.00678 ± 0.00088	2
Spectral type	K0 III	1
$v \sin i$ (km s^{-1})	4.2 ± 1.0	3
M_V (mag)	1.48 ± 0.30	1
L ($L_\odot$)	29.3 ± 8.1	1
R ($R_\odot$)	7.8 ± 1.1	1

REFERENCES.—(1) This paper; (2) Perryman 1997; (3) Fekel 1997.

90.89 days (§ 6.5), with the radius determined from its *Hipparcos* parallax, a rotational inclination of 71^{+19}_{-28} deg was found for the primary.

6.5. *Photometric Analysis*

The $V - C$ differential magnitudes in the V passband from Table 6 are plotted against Julian date in Figure 10 (*top*), and selected individual seasons are plotted in the other four panels. The results of our periodogram analyses for each season are given in Table 15. The largest amplitude (0.33 and 0.39 mag in V and B, respectively) occurred in the seventh observing season.

The means of the standard deviations of the $K - C$ differential magnitudes in column (9) of Table 15 are 0.0052 and 0.0049 mag in V and B, respectively. The standard deviations of the seasonal means of the $K - C$ magnitudes in column (8) are 0.0021 and 0.0030 mag in V and B, respectively, so we find little or no variability in either the comparison or check star on short and long timescales. The seasonal means in V are plotted in Figure 11 (*bottom*).

As seen in Figure 11 (*top*), the mean brightness of HD 217188 varies over a range of 0.27 mag in V, so there are large changes in the mean spot filling factor on a timescale of years. The second and third panels of that figure also show year-to-year variations in the photometric amplitude and period. In particular, the V amplitude varies in a fairly smooth way over a decade, but we cannot yet say whether this variation might be periodic. Similar to HD 37824 and HD 181809, there are no significant correlations between the photometric period, mean brightness, and amplitude for HD 217188, as seen in the top three panels of Figure 12.

The weighted mean of our photometric periods in Table 15 is 91.27 ± 0.12 days. Although the light curve shape of HD 217188 continually evolves and shows definite asymmetries at times, no clear secondary minima are seen in any of our yearly light curves. Times of photometric minimum derived by inspection of the light curves and converted to photometric phases with the mean 91.27 day rotation period and an arbitrary epoch are plotted in Figure 12 (*bottom*). Only a slight trend of the spots toward smaller phases is seen, since the phases were computed with our weighted-mean rotation period. All the phases of minimum lie within 0.11 phase units (rms) or 10.0 days of a

TABLE 15
RESULTS FROM PHOTOMETRIC ANALYSIS OF HD 217188

Season (1)	Photometric Band (2)	HJD Range (HJD − 2,400,000) (3)	N_{obs} (4)	$\langle V - C \rangle$ (mag) (5)	Photometric Period (days) (6)	Peak-to-Peak Amplitude (mag) (7)	$\langle K - C \rangle$ (mag) (8)	σ_{K-C} (mag) (9)
1	V	47,307–47,540	89	1.1946	93.45 ± 1.30	0.12	−0.8040	0.0051
1	B	47,309–47,537	90	1.3312	94.75 ± 1.20	0.13	−0.7134	0.0043
2	V	47,672–47,905	112	1.1748	93.76 ± 1.07	0.14	−0.8013	0.0096
2	B	47,677–47,902	113	1.3076	94.12 ± 0.83	0.14	−0.7105	0.0080
3	V	48,038–48,258	40	1.1594	86.17 ± 1.10	0.16	−0.8048	0.0058
3	B	48,043–48,258	39	1.2922	85.67 ± 1.26	0.18	−0.7135	0.0058
4	V	48,797–48,988	60	1.2262	86.47 ± 0.92	0.22	−0.7968	0.0043
4	B	48,797–48,988	62	1.3736	87.13 ± 0.98	0.25	−0.7135	0.0054
5	V	49,121–49,373	90	1.2941	89.80 ± 0.38	0.24	−0.8015	0.0048
5	B	49,124–49,373	89	1.4490	89.28 ± 0.40	0.28	−0.7043	0.0039
6	V	49,489–49,736	55	1.3197	90.83 ± 0.46	0.25	−0.8016	0.0042
6	B	49,489–49,736	55	1.4781	90.74 ± 0.44	0.29	−0.7060	0.0034
7	V	49,861–50,101	102	1.4089	88.59 ± 0.38	0.33	−0.8006	0.0038
7	B	49,867–50,101	105	1.5823	87.96 ± 0.33	0.39	−0.7063	0.0044
8	V	50,230–50,468	52	1.3442	96.49 ± 0.56	0.28:	−0.8001	0.0040
8	B	50,234–50,459	50	1.4951	97.41 ± 0.49	0.28:	−0.7080	0.0062
9	V	50,590–50,829	94	1.3270	93.66 ± 0.44	0.20	−0.8025	0.0057
9	B	50,590–50,830	92	1.4828	93.77 ± 0.49	0.22	−0.7084	0.0050
10	V	50,948–51,198	89	1.3548	92.81 ± 0.49	0.21	−0.8010	0.0043
10	B	50,949–51,198	87	1.5143	92.92 ± 0.54	0.25	−0.7077	0.0045
11	V	51,315–51,560	102	1.3153	89.97 ± 2.17	0.13	−0.7996	0.0055
11	B	51,315–51,560	99	1.4704	93.57 ± 2.67	0.17	−0.7057	0.0048
12	V	51,682–51,923	60	1.3151	95.67 ± 1.65	0.08	−0.7994	0.0045
12	B	51,682–51,923	64	1.4720	96.06 ± 1.56	0.09	−0.7069	0.0041
13	V	52,050–52,288	50	1.4257	92.35 ± 0.77	0.18	−0.7980	0.0059
13	B	52,050–52,288	52	1.6004	92.30 ± 0.87	0.23	−0.7065	0.0052
14	V	52,411–52,658	89	1.3782	...	0.04	−0.7985	0.0057
14	B	52,414–52,658	83	1.5453	...	0.05	−0.7057	0.0044
15	V	52,796–52,830	26	1.3456	...	...	−0.7999	0.0052
15	B	52,796–52,830	25	1.5093	...	...	−0.7080	0.0045

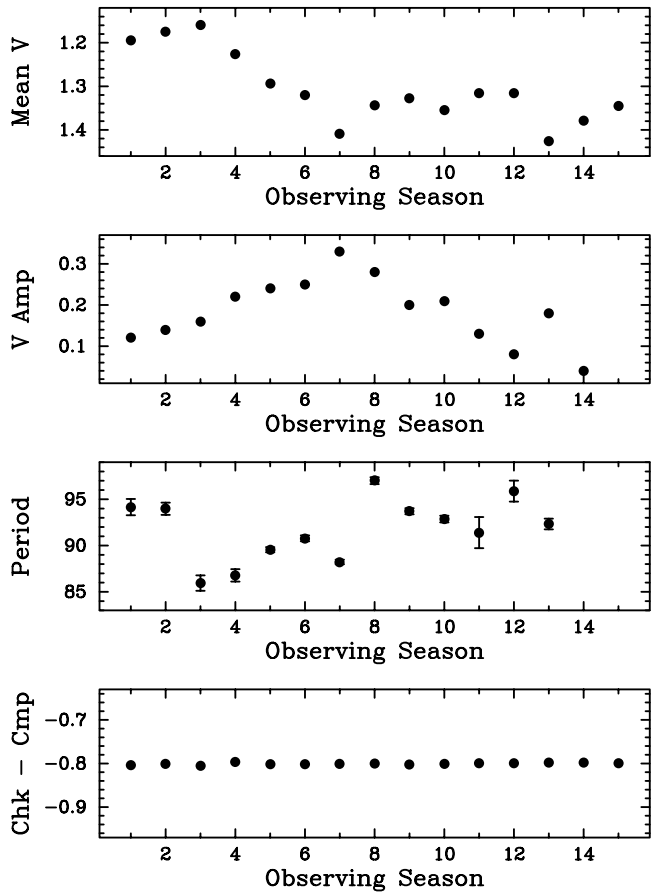

FIG. 11.—HD 217188 yearly mean differential V magnitudes (*first panel*), V amplitudes (*second panel*), photometric periods (*third panel*), and check minus comparison yearly mean differential V magnitudes (*fourth panel*), all from Table 15, plotted for each of the 15 observing seasons.

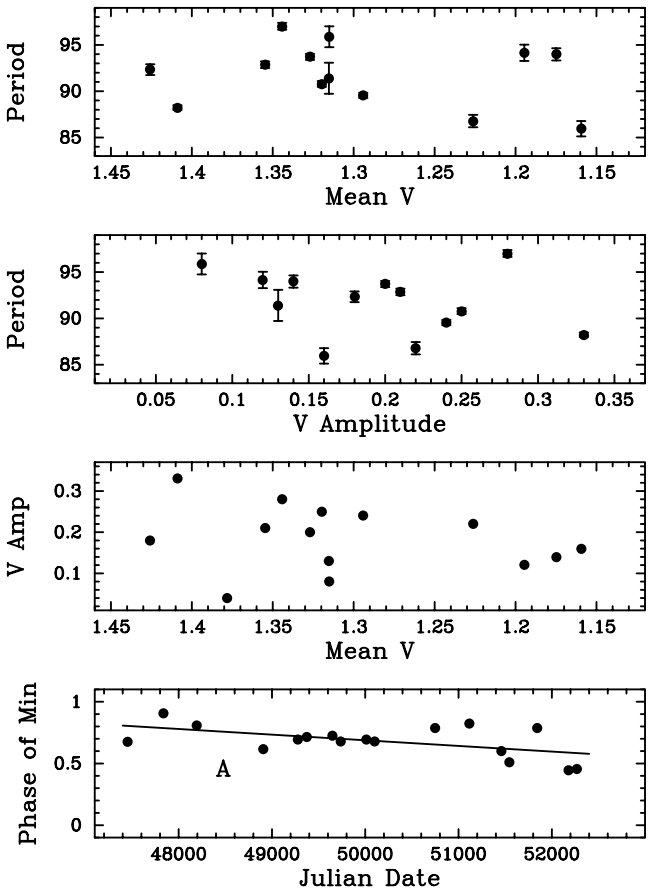

FIG. 12.—HD 217188 seasonal photometric periods plotted against yearly mean V brightness (*first panel*) and V amplitude (*second panel*), V amplitude plotted against mean brightness (*third panel*), and phases of spot minimum plotted against Julian date (*fourth panel*). No significant correlations are observed in the top three panels. The bottom panel suggests that most of the spot activity in HD 217188 occurred on a single hemisphere of the star.

single best-fit line through the observed points, which we designate as spot A. Although the rms is not as low as for HD 37824 and HD 181809, it appears that most of the spot activity in HD 217188 was concentrated on one hemisphere of the star during the span of our observations. The slope of the best-fit line corresponds to a period of 90.89 days, which we take as our best value for HD 217188's mean rotation period. Therefore, HD 217188 is rotating much slower than its 18.6 day pseudosynchronous rotation period (§ 7.1). As we discussed for HD 37824 and HD 181809, the spread in our seasonal photometric periods in Table 15 is probably not the observable result of differential rotation in HD 217188.

7. EVOLUTIONARY STATUS

7.1. *HD 37824*

The two main theories of orbital circularization and rotational synchronization (e.g., Zahn 1977; Tassoul & Tassoul 1992) disagree significantly on absolute timescales but do agree that synchronization should occur before circularization. The circular orbit of HD 37824 and the essentially synchronous rotation of its primary suggest that the K0 III star is not ascending the red giant branch for the first time, when its radius would be rapidly expanding, but rather is in the much longer lived, helium-burning core phase (Boffin et al. 1993).

Comparing the luminosity and effective temperature of HD 37824 with the solar abundance evolutionary tracks of Schaller et al. (1992) suggests a mass in the range of 1.5–2.5 $M_{\odot}$ (Fig. 13). Such a range of primary masses results in minimum secondary masses of 0.82–1.10 $M_{\odot}$. If the inclination is decreased from 90° to 60°, the range of the secondary mass is 0.95–1.27 $M_{\odot}$. Thus, from Table B1 of Gray (1992), the secondary is likely a late-F or G dwarf. Such a spectral type is consistent with the lack of detection of its lines in our red wavelength spectra.

7.2. *HD 181809*

HD 181809 has an orbital period of 13.05 days, relatively short for a system containing a giant star. However, the K-giant primary has a mean rotation period of 59.85 days (§ 5.5), and so it is quite far from synchronous rotation despite its nearly circular orbit. Strictly speaking, since the orbit is eccentric, one should not compare the rotation period with the orbital period. Hut (1981) has shown that in an eccentric orbit a star's rotational angular velocity will tend to synchronize with that of the orbital motion at periastron, a situation called pseudosynchronous rotation. However, the orbit is so close to circular that the computed pseudosynchronous period is only 1% smaller than the orbital period. The asynchronous-rotation situation of the giant primary suggests that it is on the first-ascent giant branch.

From a comparison of the luminosity and temperature of HD 181809 with the evolutionary tracks of Schaller et al. (1992) (Fig. 13), the likely mass of its primary ranges from 1.5 to 2 $M_{\odot}$. Assuming that the rotation and orbital axes are parallel and so

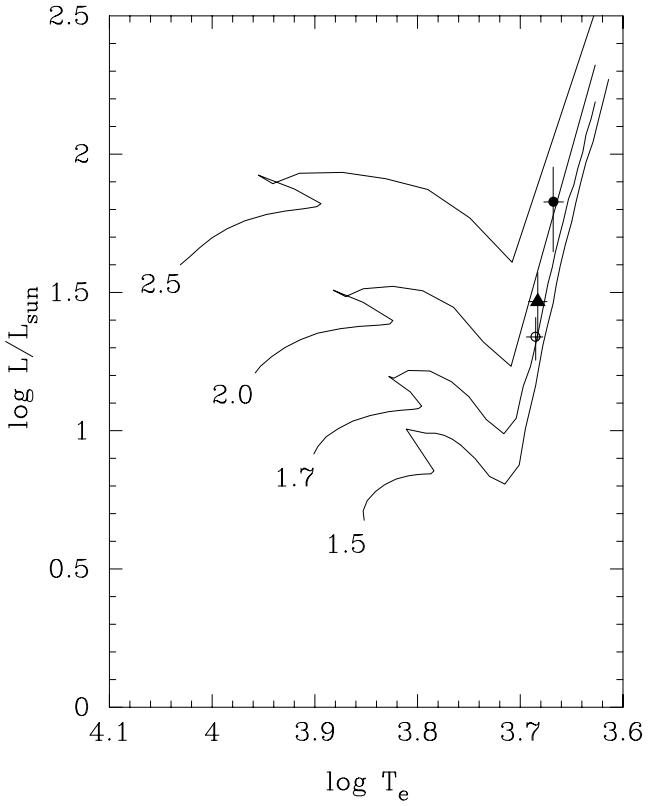

FIG. 13.—Theoretical HR diagram with the solar metallicity evolutionary tracks of Schaller et al. (1992) shown for masses between 1.5 and 2.5 $M_\odot$. Also plotted are the positions of HD 37824 (*filled circle*), HD 181809 (*open circle*), and HD 217188 (*triangle*) with their error bars.

$i = 46^\circ$, the corresponding range of secondary masses is 0.21–0.26 $M_\odot$. Thus, the secondary is most likely an M dwarf.

7.3. *HD 217188*

HD 217188 has an orbital period of 47.1 days, quite similar to that of HD 37824. However, while the orbit of HD 37824 has been circularized, that of HD 217188 has a high eccentricity of 0.47. As noted previously, rotational synchronization is predicted to occur before orbital circularization. Thus, we first examine the synchronization status of the K giant primary of HD 217188. It has a pseudosynchronous rotation period (Hut 1981) of 18.6 days compared to a mean rotation period of 90.9 days, making the star an asynchronous rotator. Such a situation is relatively common for chromospherically active giants with orbital periods greater than 1 month. Fekel & Eitter (1989) used the data from the first edition of the Catalog of Chromospherically Active Binary Stars (Strassmeier et al. 1988) to determine that about half of the systems with orbital periods between 30 and 70 days are asynchronously rotating.

For G- and K-giant binaries, Boffin et al. (1993) have estimated, from both theoretical considerations and observational data, a cutoff period of about 50 days for circularization. Orbits with periods shorter than this value are expected to have zero or near zero eccentricity. Boffin et al. (1993) concluded that stars with periods less than 50 days but with orbital eccentricities greater than about 0.1 are still on the first-ascent giant branch. Thus, the primary of HD 217188 is likely a first-ascent giant.

HD 217188 is only slightly more luminous than HD 181809, and so we again assume a mass range of 1.5–2.0 $M_\odot$ for the primary. If the rotation inclination of 71° is adopted as the orbital inclination, the secondary mass ranges from 0.24 to 0.28 $M_\odot$. Thus, it is most likely an M dwarf.

8. LITHIUM ABUNDANCES

As a result of standard theory (Iben 1967a, 1967b), it was expected that the lithium abundance of a star would be significantly diluted as it ascended the red giant branch. Observational support was provided by Brown et al. (1989), who found that in a sample of nearly 650 giants only about 2% of the stars have LTE abundances $\log \epsilon(\mathrm{Li}) \geq 1.5$. However, over the past 2 decades a small number of post–main-sequence stars have been discovered with lithium abundances significantly greater than the values predicted by standard theory. Indeed, several chromospherically active giants have lithium abundances that are equal to or greater than the initial value for Population I stars (Balachandran et al. 2000; Drake et al. 2002). Following the suggestion of Alexander (1967), Siess & Livio (1999) developed the idea that the unexpectedly high lithium abundances in some giant stars result from the accretion of planets. Alternatively, Charbonnel & Balachandran (2000) have proposed a scenario in which mixing episodes on the red giant branch and early asymptotic giant branch result in brief periods of enhanced lithium. From our spectra, Fekel & Balachandran (1994) determined logarithmic lithium abundances of 0.9, 0.5, and 0.5 for HD 37824, HD 181809, and HD 217188, respectively. Thus, these three giants are not lithium-rich but have lithium abundances that are consistent with standard theory.

9. SPOT CYCLES

As discussed above in §§ 4.5, 5.5, and 6.5, long-term variations in the mean brightness and photometric amplitude of all three stars are clearly observed in our photometric time series (Figs. 3, 7, and 11, *top two panels*), although there is little evidence for *periodic* behavior. Significant variations are also observed in the photometric periods of all three stars (Tables 9, 12, and 15; Figs. 3, 7, and 11, *third panel*), but we have argued on the basis of the coherency of the spot-migration diagrams in the bottom panels of Figures 4, 8, and 12 that these likely result from the effects of growth and decay of spots at various longitudes and not from actual changes in the rotation periods. We also found no significant correlations between the photometric period, mean brightness, and amplitude for any of the stars (Figs. 4, 8, and 12, *top three panels*). We interpret these results in the context of the random-spot model (RSM) of Eaton et al. (1996). The RSM uses large numbers (10–40) of moderately sized dark spots placed randomly on a differentially rotating star to reproduce the light curves of chromospherically active stars. The continual redistribution of spots as a result of stellar differential rotation accounts for much of the changing shape and amplitude of the light curves on rotational timescales. If the spots are also allowed to decay and appear at random on the star, with typical lifetimes of several years, then, in addition to further changes in the shape of the light curves, the RSM also predicts the kind of long-term light variations observed in most chromospherically active stars without the necessity of magnetic cycles to drive these changes. Eaton et al. (1996) demonstrated that the RSM does an excellent job of producing light curves that strongly resemble the actual light curves of chromospherically active stars on both rotational and decadal timescales. The appearances of the light curves of HD 37824, HD 181809, and HD 217188, as well as the lack of long-term periodic changes in brightness, amplitude, and period in these stars, are also consistent with the RSM. Thus, we see no clear evidence that spot cycles are occurring in these three stars.

However, the spots on HD 37824, HD 181809, and HD 217188 do not seem to be distributed randomly in longitude over the 15 year span of our photometric observations. The migration diagrams in the bottom panels of Figures 4, 8, and 12 demonstrate that the observed photometric minima in the light curves of HD 37824, HD 181809, and HD 217188 are consistent with just two, three, and one long-lived spot regions, respectively, all rotating with a constant period. The common appearance of two spot regions separated by 180° in longitude is an artifact of our simple analysis, in which we locate spots in phase from the appearance of observed minima in the light curves. Individual spot regions separated by much less than 180° will not produce resolved minima in the light curve, so we do not identify these as separate spots. The observed asymmetries in the light curves clearly demonstrate that spot groups are present at multiple longitudes. Nonetheless, the coherent spot migration diagrams argue strongly for the presence of long-lived spot regions, particularly for the largest spots plotted with filled circles in the migration diagrams, and for these long-lived regions to rotate with a constant period. This is similar to the photometric behavior seen in some other chromospherically active stars such as LQ Hya (Berdyugina et al. 2002) and FK Com (Korhonen et al. 2002). Although long-lived spot regions seem to be present in HD 37824, HD 181809, and HD 217188 so that the largest spot regions do not seem to be randomly distributed on the star during the span of our observations, the rotation periods of 53.12, 59.85, and 90.89 days are rather long compared to most chromospherically active stars. Therefore, relatively few rotation cycles are present in our data sets, and differential rotation may be less effective in breaking up and redistributing the large spot regions.

Finally, we note that the "flip-flop" effect, first discussed by Jetsu et al. (1991) in FK Com, also appears to be present in HD 37824 and HD 181809. Korhonen et al. (2002) found that FK Com shows two persistent active longitudes, separated by 180°, and that the dominant spot activity switches back and forth or flip-flops between the two longitudes. This effect has also been observed in a few other chromospherically active stars such as LQ Hya (Berdyugina et al. 2002).

The circular-orbit program provided by D. Barlow is greatly appreciated. We thank L. Boyd and D. Epand for their efforts in support of Fairborn Observatory and also D. Willmarth for his help with the coudé feed telescope at KPNO. The automated astronomy program at Tennessee State University is supported in part by NASA grant NCC5-511 and NSF grant HRD-9706268.

REFERENCES

Alexander, J. B. 1967, Observatory, 87, 238
Balachandran, S. C., Fekel, F. C., Henry, G. W., & Uitenbroek, H. 2000, ApJ, 542, 978
Balona, L. A. 1987, South African Astron. Obs. Circ., 11, 1
Barden, S. C. 1985, ApJ, 295, 162
Barker, E. S., Evans, D. S., & Laing, J. D. 1967, R. Obs. Bull., 130, 355
Batten, A. H., Fletcher, J. M., & MacCarthy, D. G. 1989, Publ. Dom. Astrophys. Obs., 17, 1
Berdyugina, S. V., Pelt, J., & Tuominen, I. 2002, A&A, 394, 505
Bidelman, W. P. 1981, AJ, 86, 553
———. 1985, AJ, 90, 341
Bidelman, W. P., & MacConnell, D. J. 1973, AJ, 78, 687
Boffin, H. M. J., Cerf, N., & Paulus, G. 1993, A&A, 271, 125
Bopp, B. W. 1984, ApJS, 54, 387
Boyd, L. J., Genet, R. M., Hall, D. S., & Henry, G. W. 1985, Inf. Bull. Variable Stars, 2727, 1
Brown, J. A., Sneden, C., Lambert, D. L., & Dutchover, E. 1989, ApJS, 71, 293
Buckley, D. A. H., Tuohy, I. R., Remillard, R. A., Brant, H. V., & Schwartz, D. A. 1987, ApJ, 315, 273
Charbonnel, C., & Balachandran, S. C. 2000, A&A, 359, 563
Collier Cameron, A. 1987, South African Astron. Obs. Circ., 11, 13
Cutispoto, G., Pastori, L., Tagliaferri, G., Messina, S., & Pallavicini, R. 1999, A&AS, 138, 87
Cutispoto, G., Tagliaferri, G., Giommi, P., Gouiffes, C., Pallavicini, R., Pasquini, L., & Rodono, M. 1991, A&AS, 87, 233
De Medeiros, J. R., & Udry, S. 1999, A&A, 346, 532
Dempsey, R. C., Linnsky, J. L., Fleming, T. A., & Schmitt, J. H. M. M. 1993, ApJS, 86, 599
Drake, N. A., de la Reza, R., da Silva, L., & Lambert, D. L. 2002, AJ, 123, 2703
Eaton, J. A., Henry, G. W., & Fekel, F. C. 1996, ApJ, 462, 888
———. 2003, in The Future of Small Telescopes in the New Millennium, Vol. 2, ed. T. D. Oswalt (Dordrecht: Kluwer), 189
Fekel, F. C. 1997, PASP, 109, 514
Fekel, F. C., & Balachandran, S. 1994, in ASP Conf. Ser. 64, Cool Stars Stellar Systems and the Sun, ed. J.-P. Caillault (San Francisco: ASP), 279
Fekel, F. C., & Eitter, J. J. 1989, AJ, 97, 1139
Fekel, F. C., Henry, G. W., Eaton, J. A., Sperauskas, J., & Hall, D. S. 2002, AJ, 124, 1064
Fekel, F. C., Moffett, T. J., & Henry, G. W. 1986, ApJS, 60, 551
Fekel, F. C., Strassmeier, K. G., Weber, M., & Washuettl, A. 1999, A&AS, 137, 369
Fitzpatrick, M. J. 1993, in ASP Conf. Ser. 52, Astronomical Data Analysis Software and Systems II, ed. R. J. Hanisch, R. V. J. Brissenden, & J. Barnes (San Francisco: ASP), 472
Fleming, T. A., Gioia, I. M., & Maccacaro, T. 1989, AJ, 98, 692
Flower, P. J. 1996, ApJ, 469, 355
Gray, D. F. 1992, The Observation and Analysis of Stellar Photospheres (Cambridge: Cambridge Univ. Press)
Hall, D. S., Fekel, F. C., Henry, G. W., & Barksdale, W. S. 1991, AJ, 102, 1808
Hall, D. S., Henry, G. W., Louth, H., & Renner, T. R. 1983, Inf. Bull. Var. Stars, 2409, 1
Helfand, D. J., Schnee, S., Becker, R. H., White, R. L., & McMahon, R. G. 1999, AJ, 117, 1568
Henry, G. W. 1995a, in ASP Conf. Ser. 79, Robotic Telescopes: Current Capabilities, Present Developments, and Future Prospects for Automated Astronomy, ed. G. W. Henry & J. A. Eaton (San Francisco: ASP), 37
———. 1995b, in ASP Conf. Ser. 79, Robotic Telescopes: Current Capabilities, Present Developments, and Future Prospects for Automated Astronomy, ed. G. W. Henry & J. A. Eaton (San Francisco: ASP), 44
———. 1999, PASP, 111, 845
Henry, G. W., Fekel, F. C., Henry, S. M., & Hall, D. S. 2000, ApJS, 130, 201
Henry, T. J., Soderblom, D. R., Donahue, R. A., & Baliunas, S. L. 1996, AJ, 111, 439
Hooten, J. T., & Hall, D. S. 1990, ApJS, 74, 225
Houk, N., & Smith-Moore, M. 1988, Michigan Spectral Catalogue, Vol. 4 (Ann Arbor: Univ. Michigan), 350
Houk, N., & Swift, C. 1999, Michigan Spectral Catalogue, Vol. 5 (Ann Arbor: Univ. Michigan), 333
Huenemoerder, D. P., & Barden, S. C. 1984, BAAS, 16, 510
Hut, P. 1981, A&A, 99, 126
Iben, I. 1967a, ApJ, 147, 624
———. 1967b, ApJ, 147, 650
Jeffries, R. D., Bertram, D., & Spurgeon, B. R. 1995, MNRAS, 276, 397
Jetsu, L., Pelt, J., Tuominen, I., & Nations, H. 1991, in IAU Colloq. 130, The Sun and Cool Stars: Activity, Magnetism, Dynamos, ed. I. Tuominen, D. Moss, & G. Rüdiger (Springer: Heidelberg), 381
Keenan, P. C., & McNeil, R. C. 1989, ApJS, 71, 245
Korhonen, H., Berdyugina, S. V., & Tuominen, I. 2002, A&A, 390, 179
Lloyd Evans, T., & Koen, M. C. J. 1987, South African Astron. Obs. Circ., 11, 21
Lucy, L. B., & Sweeney, M. A. 1971, AJ, 76, 544
Mitrou, C. K., Mathioudakis, M., Doyle, J. G., & Antonopoulou, E. 1997, A&A, 317, 776
Morel, T., Micela, G., Favata, F., & Katz, D. 2004, A&A, 426, 1007
Morel, T., Micela, G., Favata, F., Katz, D., & Pillitteri, I. 2003, A&A, 412, 495
Morris, D. H., & Mutel, R. L. 1988, AJ, 95, 204
Neuhaüser, R., Torres, G., Sterzik, M. F., & Randich, S. 1997, A&A, 325, 647
O'Neal, D., Saar, S., & Neff, J. E. 1996, ApJ, 463, 766
Perryman, M. A. C., ed. 1997, The *Hipparcos* and Tycho Catalogues (ESA SP-1200) (Noordwijk: ESA)
Randich, S., Giampapa, M. S., & Pallavicini, R. 1994, A&A, 283, 893

Randich, S., Gratton, R., & Pallavicini, R. 1993, A&A, 273, 194
Scarfe, C. D., Batten, A. H., & Fletcher, J. M. 1990, Publ. Dominion Astrophys. Obs., 18, 21
Schaller, G., Schaerer, D. Meynet, G., & Maeder, A. 1992, A&AS, 96, 269
Schwope, A. D., et al. 2000, Astron. Nachr., 321, 1
Siess, L., & Livio, M. 1999, MNRAS, 308, 1133
Slee, O. B., Nelson, G. J., Stewart, R. T., Wright, A. E., Innis, J. L., Ryan, S. G., & Vaughan, A. E. 1987, MNRAS, 229, 659
Strassmeier, K. G., & Fekel, F. C. 1990, A&A, 230, 389
Strassmeier, K. G., Hall, D. S., Boyd, L. J., & Genet, R. M. 1989, ApJS, 69, 141
Strassmeier, K. G., Hall, D. S., Fekel, F. C., & Scheck, M. 1993, A&AS, 100, 173
Strassmeier, K. G., Hall, D. S., Zeilik, M., Nelson, E., Eker, Z., & Fekel, F. C. 1988, A&AS, 72, 291
Strassmeier, K. G., Washuettl, A., Granzer, T., Scheck, M., & Weber, M. 2000, A&AS, 142, 275
Tagliaferri, G., Cutispoto, G., Pallivicini, R., Randich, S., & Pasquini, L. 1994, A&A, 285, 272
Tassoul, J.-L., & Tassoul, M. 1992, ApJ, 395, 259
Taylor, B. J. 1999, A&AS, 134, 523
Wolfe, R. H., Horak, H. G., & Storer, N. W. 1967, in Modern Astrophysics, ed. M. Hack (New York: Gordon & Breach), 251
Zahn, J.-P. 1977, A&A, 57, 383

Note added in proof.—We have recently obtained additional photometric observations of HD 38309, our comparison star for HD 37824. We have found HD 38309 to be a γ Doradus pulsator with an amplitude of a few millimags. The slight variability in the $K - C$ seasonal means shown in Figure 3 (*bottom*) is probably the result of slow brightness changes in the check star HD 37984 (K1 III). Thus, both our comparison and check stars are low-amplitude variables. However, these slight variations do not affect the results of our analysis of the much larger variability in HD 37824.